0026-895X/01/6001-1–19$3.00
MOLECULAR PHARMACOLOGY
Copyright © 2001 The American Society for Pharmacology and Experimental Therapeutics
Mol Pharmacol 60:1–19, 2001

Vol. 60, No. 1
878/913675
Printed in U.S.A.

MINIREVIEW

Structural Mimicry in G Protein-Coupled Receptors: Implications of the High-Resolution Structure of Rhodopsin for Structure-Function Analysis of Rhodopsin-Like Receptors

JUAN A. BALLESTEROS, LEI SHI, and JONATHAN A. JAVITCH

Novasite Pharmaceuticals, Inc. (J.A.B.), San Diego, California; Center for Molecular Recognition (L.S., J.A.J.) and Departments of Psychiatry (J.A.J.) and Pharmacology (L.S., J.A.J.), Columbia University College of Physicians and Surgeons, New York, New York

Received February 12, 2001; accepted April 10, 2001

This paper is available online at http://molpharm.aspetjournals.org

ABSTRACT

The availability of a high-resolution structure of rhodopsin now allows us to reconsider research attempts to understand structure-function relationships in other G protein-coupled receptors (GPCRs). A comparison of the rhodopsin structure with the results of previous sequence analysis and molecular modeling that incorporated experimental results demonstrates a high degree of success for these methods in predicting the helix ends and protein-protein interface of GPCRs. Moreover, the amino acid residues inferred to form the surface of the binding-site crevice based on our application of the substituted-cysteine accessibility method in the dopamine D_2 receptor are in remarkable agreement with the rhodopsin structure, with the notable exception of some residues in the fourth transmembrane segment. Based on our analysis of the data reviewed, we propose that the overall structures of rhodopsin and of amine receptors are very similar, although we also identified localized regions where the structure of these receptors may diverge. We further propose that several of the highly unusual structural features of rhodopsin are also present in amine GPCRs, despite the absence of amino acids that might have thought to have been critical to the adoption of these features. Thus, different amino acids or alternate microdomains can support similar deviations from regular α-helical structure, thereby resulting in similar tertiary structure. Such structural mimicry is a mechanism by which a common ancestor could diverge sufficiently to develop the selectivity necessary to interact with diverse signals, while still maintaining a similar overall fold. Through this process, the core function of signaling activation through a conformational change in the transmembrane segments that alters the conformation of the cytoplasmic surface and subsequent interaction with G proteins is presumably shared by the entire Class A family of receptors, despite their selectivity for a diverse group of ligands.

G protein-coupled receptors (GPCRs) represent a very large superfamily of receptors that are critical for signaling of a diverse group of ligands to heterotrimeric G proteins (Gether, 2000). Ligands for these receptors include light, odorants, tastes, small molecule neurotransmitters, peptides, glycoprotein hormones, proteases, and others. Despite an enormous amount of research on the structure and function of these receptors, until very recently, no high-resolution structure of any G protein-coupled receptor was available. Inferences about the structure of these receptors have been based on critical cryomicroscopy studies of rhodopsin that indicated the existence of seven transmembrane segments

This work was supported in part by National Institutes of Health Grants MH57324 and MH54137 and the Lebovitz Trust.

J.A.B. and L.S. contributed equally to this work and are listed in alphabetical order.

ABBREVIATIONS: GPCRs, G protein coupled receptors; TM, transmembrane segment; SASA, solvent accessible surface area; SCAM, substituted-cysteine accessibility method; MTS, methanethiosulfonate; RMSD, root mean square distance; IpBABC, *p*-(bromoacetamido)benzyl-1-[^{125}I]iodocarazolol; E2, second extracellular loop; MD, molecular dynamics. Receptor abbreviations: 5H1A (5H1B, 5H2A), 5-hydroxytryptamine 1A (1B, 2A) receptor; A1AA (A1AB, A2AA), α1A (1B, 2A) adrenergic receptor; AA1R (AA2A), adenosine A1 (A2A) receptor; ACM1 (ACM2, ACM3, ACM5), muscarinic acetylcholine M1 (M2, M3, M5) receptor; ACTR, adrenocorticotropin receptor; AG2R, type-1 angiotensin II receptor; B2AR, β_2 adrenergic receptor; D2DR, dopamine D2 receptor; ETBR, endothelin B receptor; ET1R, endothelin-1 receptor; GASR, gastrin/cholecystokinin type B receptor; GRHR, gonadotropin-releasing hormone receptor; HH2R, histamine H2 receptor; MSHR, melanocyte stimulating hormone receptor; NK1R, substance-P receptor; NK2R, substance-K receptor; NTR1, neurotensin type I receptor; OPRK, κ-type opioid receptor; OPSD, rhodopsin; P2UR, P2U purinoceptor 1; P2YR, P2Y purinoceptor 1; PAFR, platelet activating factor receptor; TSHR, thyrotropin receptor.

(TMs) and gave an indication of the relative disposition of these TMs (Unger et al., 1997). Molecular models of rhodopsin and other GPCRs have been built based on this low-resolution structure, on additional experimental data pertinent to structure, and on inferences from sequence alignments, analyzed in terms of conservation and physicochemical properties (Ballesteros and Weinstein, 1995; Baldwin et al., 1997; Visiers et al., 2001). The crystal structure of bovine rhodopsin was recently determined to 2.8 Å (Palczewski et al., 2000). This landmark accomplishment provides a timely opportunity to review and reconsider previous attempts to infer, through indirect means, the structure of GPCRs. By analyzing the consistency of previous data from a number of different GPCRs with the recent structure of rhodopsin, we consider to what extent the structure of other GPCRs is likely to resemble the structure of rhodopsin. In this review, we focus such a comparison on previous studies of amine GPCRs, with special emphasis on our work on the dopamine D_2 receptor.

The sequence identity between bovine rhodopsin and the human dopamine D_2 receptor is ~19% overall and ~25% in the transmembrane domains. In the case of soluble proteins, for which vastly more structural data is available, there is a clear structural similarity between proteins with >~25% sequence identity, but below this level of sequence identity, structural divergence increases dramatically (Wilson et al., 2000; Yang and Honig, 2000a). Nonetheless, recent work has suggested that a number of different soluble proteins can achieve the same fold with different sequence patterns (Russell and Barton, 1994; Jornvall et al., 1995; Mirny and Shakhnovich, 1999; Yang and Honig, 2000b). The extent of structural similarity between rhodopsin and other GPCRs is not known, and we are currently limited to only one high-resolution structure from this entire superfamily of receptors. Although the presence of a number of highly conserved residues makes it possible to align the TM residues of the class A receptors (Fig. 1), these domains differ at ~75% of the TM positions. In a number of cases these differences are dramatic, such as the presence or absence of a Pro in a TM.

Nonetheless, based on our analysis of the data to be reviewed here, the overall structures of the transmembrane domains of rhodopsin and of amine receptors may be remarkably similar. We further propose that several of the highly unusual structural features of rhodopsin are also present in amine GPCRs, despite the absence of amino acids that might have been thought to be critical for the adoption of these features. Thus, through a form of *structural mimicry*, we propose that different amino acids or alternate microdomains can support similar local deviations from regular α-helical structure, thereby resulting in very similar tertiary structures. Thus, by structural mimicry, a common ancestor could diverge sufficiently to develop the selectivity necessary to interact with diverse signals but still maintain a similar overall fold and the core function of signaling activation through a conformational change in the TMs that alters the conformation of the cytoplasmic surface and subsequent interaction with G proteins.

Transmembrane Helix Ends and Orientation

The helical net diagram of rhodopsin in Fig. 2A shows the residues comprising the solvent accessible surface area (SASA) calculated from the high-resolution structure of rhodopsin. In such a calculation, a sphere the size of a water molecule is rolled along the entire receptor and the accessible surface is quantified (Lee and Richards, 1971; Shrake and Rupley, 1973). Because the crystal structure did not resolve lipid or detergent, within the transmembrane helical domains, the surface with the greatest calculated surface accessibility is the portion of rhodopsin that is normally exposed to lipid. In Fig. 2A, the most accessible residues are shown with blue circles, and the most inaccessible are shown with red circles. Superimposed on these nets (Fig. 2, A and B) are prior predictions regarding the lipid exposure of residues in amine receptors (Ballesteros and Weinstein, 1995; Visiers et al., 2001). Residues in the surface predicted to face lipid are shown in blue letters, and residues predicted to face the protein interior and/or the binding-site crevice are shown in red letters. These predictions were based upon the pattern of conservation of various physicochemical properties of the amino acid side chains within this family of receptors, complemented by results from experimental probing in various GPCRs. Except for the extracellular portion of TM1 and some residues in TM4, the predictions are remarkably consistent with the calculated SASA from the rhodopsin structure, suggesting the utility and reliability of these methods of analysis and prediction of structural features, as well as the overall structural similarity among Class A receptors. Overall, 91% of the residues with low SASA (<10%) were predicted to face the interior of the TM helix bundle, whereas 78% of the residues with high SASA (>15%) were predicted to face lipid. Whereas the divergence of the predictions from the SASA in TM1 may relate to real differences in the structure in this region because of the nonconserved Pro, the disagreement in TM4 is more challenging, as will be discussed below.

The boundaries of the interface between the membrane and aqueous environment inferred from electron paramagnetic resonance spectroscopy studies of spin-labeled Cys substituted for residues at the cytoplasmic ends of each TM of rhodopsin (Farahbakhsh et al., 1995; Altenbach et al., 1996, 1999a,b) are very consistent with the cytoplasmic ends of the seven TM α-helices in the high-resolution structure of rhodopsin (Palczewski et al., 2000). As shown in the dotted circles in Fig. 2A, however, the spin-labeling studies predicted a continuation of α-helical conformation for one to three turns at the cytoplasmic ends of TM5, TM6, and TM7 within the aqueous milieu. Remarkably, these residues are clearly not in an α-helical conformation in the rhodopsin structure, with Ψ values dramatically out of the permitted range. Although there are a number of technical differences between these studies, such as the differing detergent environments and the use of Cys mutants, another possible explanation for the discrepancy is that this region is dynamic and that a substantial conformational reorganization may be critical to receptor activation and G protein interaction. That the region from $Gln236^{6.19}$ to $Glu239^{6.22}$ was not resolved in the rhodopsin crystal structure also suggests that this region is highly dynamic even in the inactive state, and the high average B values in the resolved third intracellular loop are also consistent with such an interpretation.

Predictions of the helix ends are shown in Fig. 2B (Ballesteros and Weinstein, 1995; Visiers et al., 2001). Interestingly, at the cytoplasmic ends these predictions are more consistent with the results of the spin-labeling studies than with the actual rhodopsin structure (Fig. 2). At the extracellular side,

both the predictions and substituted-cysteine accessibility method (SCAM) studies (see below) proposed helical ends that were either in agreement with or shorter than the rhodopsin structure. A possible explanation for these discrepancies is illustrated in Fig. 3A, in which rhodopsin is illustrated embedded in its natural environment, phospholipid molecules. As demonstrated by White and Wimley (1999), the membrane is not a homogenous hydrophobic layer; instead, it consists of a relatively constant, low dielectric region, approximately 30 Å, sandwiched between two complex regions of variable dielectric behavior, both of which are approximately 15 Å. The 30-Å core region corresponds to the hydrophobic lipid chains, whereas the surrounding 15-Å regions correspond to the mixed hydrophobic/hydrophilic phase formed by the phospholipid headgroup domains.

That approximately 40% of the transmembrane domain interacts with the phospholipid headgroups (Fig. 3A) is surprising, given that the literature on GPCRs, and most prediction methods, tends to equate the membrane with the hydrophobic phase. Indeed, the most common methods used to predict membrane-spanning helices have been the hydrophobicity plot, which identifies segments with an overall high hydrophobicity, and hydrophobic moment, which estimates the amphiphilic character of a helical segment (α-helix with two faces, one more polar and another more hydrophobic). Because the helical turn facing the lipid headgroups is composed of polar residues on both sides of the helix, both methods will fail to predict these helical turns (Ballesteros and Weinstein, 1995; Visiers et al., 2001). On the extracellular side, residues facing the interior of the helical bundle at the level of the lipid headgroup region are likely to participate in ligand recognition and thus are divergent through evolution, so methods based on sequence conservation may also fail to predict the extracellular end of helical segments. Thus, we should expect the predicted helical ends at the extracellular side to be minimal ends.

At the cytoplasmic side of the TMs, prediction methods based on the hydrophobic plot or moment will also fail to recognize the helical turns within the phospholipid headgroups. Arg and Lys concentrate at the cytoplasmic boundary of membrane proteins, on one face of the helix, where they interact with the lipid at the level of the phospholipid headgroups (Ballesteros and Weinstein, 1992, 1995; Visiers et al., 2001). This is illustrated in Fig. 3A, in which the positively charged side chains of the Arg and Lys residues in rhodopsin are positioned to participate in favorable ionic interactions with the negatively charged phospholipid headgroups. In amine GPCRs, the cytoplasmic boundaries of the TMs contain approximately three times as many basic residues (Arg and Lys) as acidic residues (Asp and Glu), thereby resulting in a significant positive charge at the cytoplasmic boundary of these receptors. This observation correlates with the known preponderance of negatively charged phospholipid headgroups in the cytoplasmic leaflet of eukaryotic plasma membranes. Thus, despite the absence of conservation of the exact position of these Arg/Lys in GPCRs, they are consistently present throughout evolution in the same TM helices, at the cytoplasmic boundaries where they face the lipid headgroups. What is conserved is their general location and presumed structural/functional role.

The positions of these Arg/Lys can be used to predict the cytoplasmic ends of the TM helices (Ballesteros and Wein-

```
     1.30
bOPSD  35 WQFSMLAAYMFLLIMLGFPINFLTLYVTVQHKKLR
hD2DR  32 PHYNYYATLLTLLIAVIVFGNVLVCMAVSREKALQ
hB2AR  31 VWVVGMGIVMSLIVLAIVFGNVLVITAIAKFERLQ
hACM1  23 WQVAFIGITTGLLSLATVTGNLLVLISFKVNTELK
hOPRK  57 AIPVIITAVYSVVFVVGLVGNSLVMFVIIRYTKMK
hNK1R  30 WQIVLWAAAYTVIVVTSVVGNVVVMWIILAHKRMR
hTSHR 412 MGYKFLRIVVWFVSLLALLGNVFVLLILLTSHYKL
     2.38
bOPSD  71 PLNYILLNLAVADLFMVFGGFTTTLYTSLH
hD2DR  68 TTNYLIVSLAVADLLVATLVMPWVVYLEVV
hB2AR  67 VTNYFITSLACADLVMGLAVVPFGAAHILM
hACM1  59 VNNYFLLSLACADLIIGTFSMNLYTTYLLM
hOPRK  93 ATNIYIFNLALADALVTTTMPFQSTVYLMN
hNK1R  66 VTNYFLVNLAFAEASMAAFNTVVNFTYAVH
hTSHR 448 VPRFLMCNLAFADFCMGMYLLLIASVDLYT
     3.22
bOPSD 107 PTGCNLEGFFATLGGEIALWSLVVLAIERYVVVCK
hD2DR 104 RIHCDIFVTLDVMMCTASILNLCAISIDRYTAVAM
hB2AR 103 NFWCEFWTSIDVLCVTASIETLCVIAVDRYFAITS
hACM1  95 TLACDLWLALDYVASNASVMNLLLISFDRYFSVTR
hOPRK 128 DVLCKIVISIDYYNMFTSIFTLTMMSVDRYIAVCH
hNK1R 102 LFYCKFHNFFPIAAVFASIYSMTAVAFDRYMAIIH
hTSHR 491 GPGCNTAGFFTVFASELSVYTLTVITLERWYAITF
     4.38
bOPSD 149 GENHAIMGVAFTWVMALACAAPPLV
hD2DR 148 SKRRVTVMISIVWVLSFTISCPLLF
hB2AR 146 TKNKARVIILMVWIVSGLTSFLPIQ
hACM1 138 TPRRAALMIGLAWLVSFVLWAPAIL
hOPRK 171 TPLKAKIINICIWLLSSSVGISAIV
hNK1R 143 SATATKVVICVIWVLALLLAFPQGY
hTSHR 534 RLRHACAIMVGGWVCCFLLALLPLV
     5.35
bOPSD 200 NESFVIYMFVVHFIIPLIVIFFCYGQLVFTVKEAAAQQ
hD2DR 186 NPAFVVYSSIVSFYVPFIVTLLVYIKIYIVLRRRRKRV
hB2AR 196 NQAYAIASSIVSFYVPLVIMVFVYSRVFQEAKRQLQKI
hACM1 185 QPIITFGTAMAAFYLPVTVMCTLYWRIYRETENRAREL
hOPRK 223 DLFMKICVFIFAFVIPVLIIIVCYTLMILRLKSVRLLS
hNK1R 193 EKVYHICVTVLIYFLPLLVIGYAYTVVGITLWASEIPG
hTSHR 562 SYAKVSICLPMDTETPLALAYIVFVLTLNIVAFVIVCC
     6.23
bOPSD 240 SATTQKAEKEVTRMVIIMVIAFLICWLPYAGVAFYIFT
hD2DR 361 RKLSQQKEKKATQMLAIVLGVFIICWLPFFITHILNIH
hB2AR 261 SSKFCLKEHKALKTLGIIMGTFTLCWLPFFIVNIVHVI
hACM1 353 KTFSLVKEKKAARTLSAILLAFILTWTPYNIMVLVSTF
hOPRK 262 SREKDRNLRRITRLVLVVVAVFVVCWTPIHIFILVEAL
hNK1R 236 YHEQVSAKRKVVKMMIVVVCTFAICWLPFHIFFLLPYI
hTSHR 612 QYNPGDKDTKIAKRMAVLIFTDFICMAPISFYALSAIL
     7.33
bOPSD 286 IFMTIPAFFAKTSAVYNPVIYIMMNKQFRNCMVTTLCC
hD2DR 406 VLYSAFTWLGYVNSAVNPIIYTTFNIEFRKAFLKILHC
hB2AR 306 EVYILLNWIGYVNSGFNPLIYCRS-PDFRIAFQELLCL
hACM1 398 TLWELGYWLCYVNSTINPMCYALCNKAFRDTFRLLLLC
hOPRK 310 SSYYFCIALGYTNSSLNPILYAFLDENFKRCFRDFCFP
hNK1R 285 QVYLAIMWLAMSSTMYNPIIYCCLNDRFRLGFKHAFRC
hTSHR 658 NSKILLVLFYPLNSCANPFLYAIFTKAFQRDVFILLSK
```

Fig. 1. Sequence alignment of the transmembrane domain and relevant adjacent residues in selected receptors. Yellow represents residues in the dopamine D_2 receptor found in SCAM studies to be accessible and protected. Orange represents accessible residues that were not protected or for which protection was not measured because of small effect size. The superscored regions represent the α-helical domains in rhodopsin. The most conserved residues (X.50) in each TM are indicated by arrows, and the index number of the first residue in each TM of the alignment is indicated. The residue numbers of the first residues in each TM of each indicated receptor are shown to the right of the receptor names. Receptor names are abbreviated according to their SWISS-PROT Annotated Protein Sequence Database entry names: http://www.expasy.ch/cgi-bin/lists?7tmrlist.txt. h, human; b, bovine.

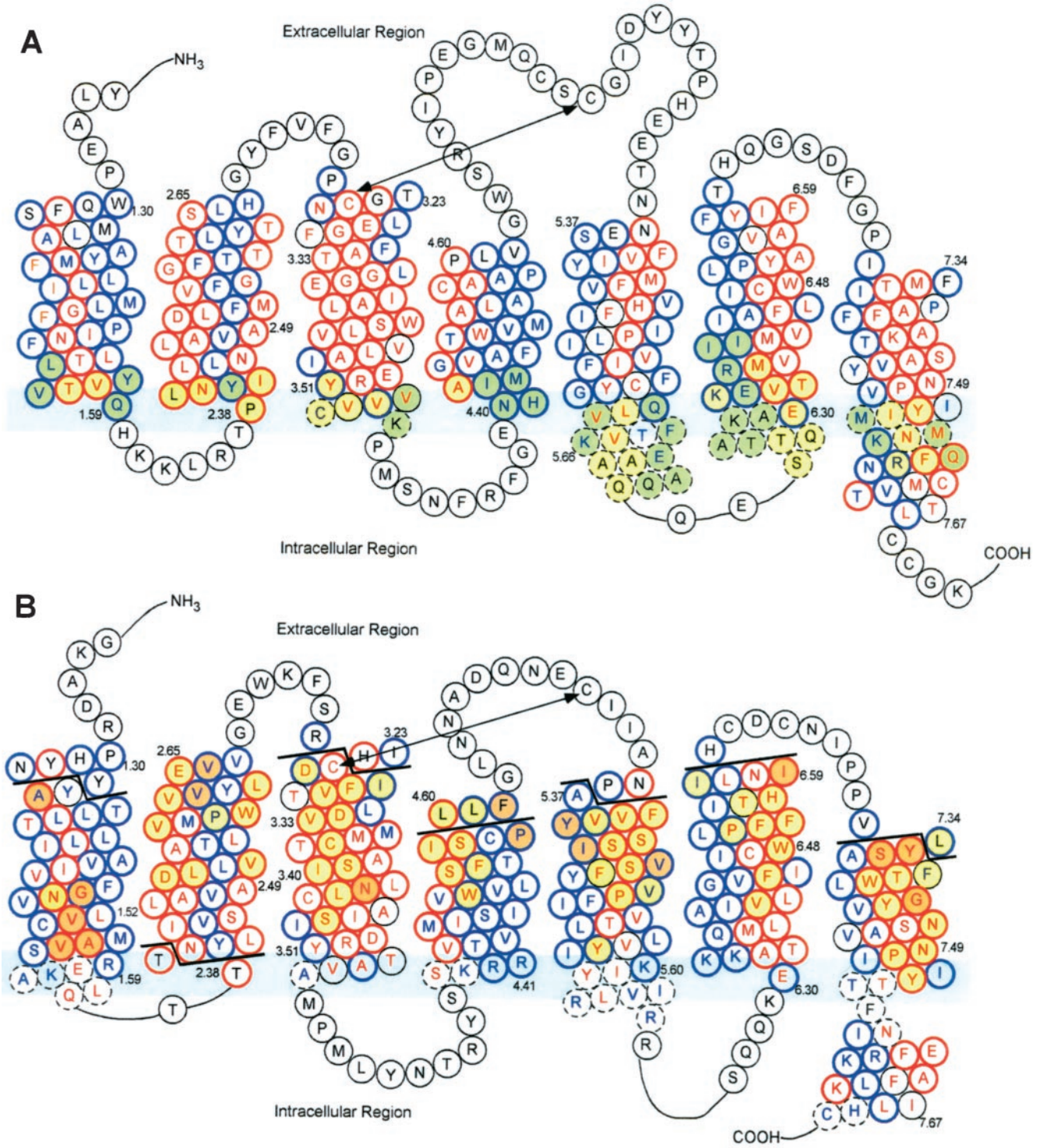

Fig. 2. Helical net representations depicting the relative positions of the residues in the transmembrane domain of rhodopsin (A) and the dopamine D_2 receptor (B). Residues with a calculated SASA of less than 10% in the bovine rhodopsin structure are indicated with red circles and those with SASA greater than 15% are indicated with blue circles. The single letter amino acid code is shown in red for residues aligned with those in amine receptors that were predicted to face the interior of the TM helix bundle (see text), and in blue for those that were predicted to face lipid. The helix ends are shown as per the rhodopsin structure. The cytoplasmic lipid/hydrophilic interface is shown by light blue stripes. A, bovine rhodopsin. Based on spin-labeling experiments, the residues with yellow shading face the protein interior, whereas those with green shading face lipid (see text). Residues at the cytoplasmic ends of TM5, TM6, and TM7 predicted by these spin-labeling studies to be in an α-helical conformation but which are not in an α-helical conformation in the rhodopsin structure are shown with dotted circles. B, human dopamine D_2 receptor, with the rhodopsin SASA and amine receptor predictions shown as in A. The residues with yellow shading are accessible and protected in SCAM experiments in the D_2 receptor, whereas those with orange shading were not protected or protection was not tested because of small effect size (see text). Tyr192$^{5.41}$, Ile195$^{5.44}$, and Val196$^{5.45}$ in TM5 are shown in orange, even though they are accessible and protected, because they are not accessible in the β_2 adrenergic receptor (see text). Residues at the ends of TMs predicted to be in an α-helical conformation but which are not in an α-helical conformation in the rhodopsin structure are shown with dotted circles; residues in an α-helical conformation in the rhodopsin structure but not predicted to be in an α-helical conformation are demarcated from the TMs by solid lines.

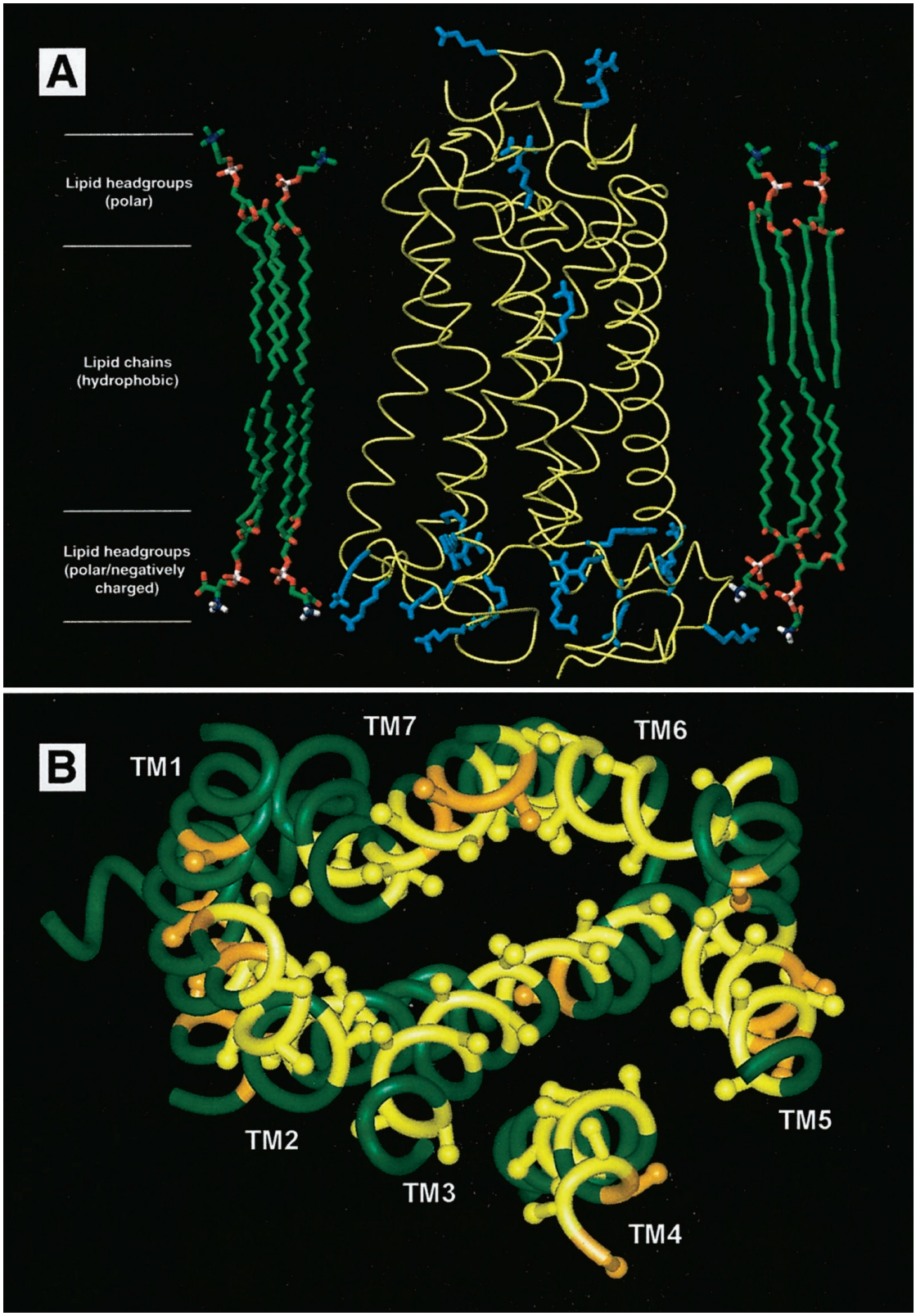

Fig. 3. A, three-dimensional molecular representation of the distribution of positively charged residues in rhodopsin. The Cα trace of rhodopsin (yellow) is viewed perpendicular to the transmembrane domain axis, with the extracellular side on the top and the intracellular side on the bottom. The side chains of Arg and Lys are shown in blue sticks. To represent the membrane bilayer, several phospholipid molecules (phosphatidylcholines in the extracellular leaflet and negatively charged phosphatidylserines in the cytoplasmic leaflet) are shown. B, three-dimensional molecular representations of the transmembrane domain viewed extracellularly, showing the Cα traces from the high-resolution structure of bovine rhodopsin. The Cβ and the bond between Cα and Cβ are shown for those residues for which the aligned residues in the dopamine D_2 receptor are accessible. Yellow represents protected residues, and orange represents residues that are accessible but not protected, or for which protection was not tested because of small effect size. The remaining residues in the TMs are shown in green without Cβ.

stein, 1995; Visiers et al., 2001). Notably, these predictions of the cytoplasmic helical ends and a recent revision thereof (Jensen et al., 2000) agree extremely well with the spin-labeling studies in rhodopsin, even though the inferred ends for TM5, TM6, and TM7 are longer than the current rhodopsin structure. As discussed above, this might be explained by protein dynamics. It is also possible, however, that in the crystal structure (because the environment of these Arg/Lys-rich cytoplasmic segments lack negatively charged phospholipid headgroups and thus may not mimic the native environment), the result might be dynamic, unstable, or unfolded helical ends at the cytoplasmic boundaries in the structure.

In addition to its structural significance, the portions of the receptor embedded in the phospholipid headgroup regions perform critical functional roles. On the extracellular side, ligand passes through and binds to the portion of the receptor that resides in the headgroup region, as demonstrated for the TRH receptor (Colson et al., 1998). Furthermore, there are an increasing number of GPCR ligands that have been shown to partition from the aqueous medium into the phospholipid headgroup region and then to diffuse across the membrane to bind to the receptor. Examples of such a mode of binding include lipid-like ligands such as cannabinoids (Yang et al., 1992), less hydrophobic compounds, such as opioid receptor ligands (Schwyzer, 1995), and the PACAP peptide ligand (Inooka et al., 2001), and it is possibly a much more widespread mechanism of binding than anticipated.

At the cytoplasmic boundary, the receptor domains embedded in the phospholipid headgroup region contain the key residues inferred to interact with G-proteins. Lipid modification of G-proteins positions them within the phospholipid headgroup region as well. Thus the mixed hydrophilic/hydrophobic phospholipid headgroup regions provide an environment that may support the key interactions of GPCRs with ligands from the extracellular side and with G-proteins and other interacting proteins, such as receptor kinases, from the cytoplasmic side. From this perspective, the hydrophobic core of the membrane formed by the lipid side chains would be responsible for transducing the signal across the membrane, from ligand binding to conformational changes at the cytoplasmic boundaries that facilitate G protein coupling.

The Substituted-Cysteine Accessibility Method

We have used the substituted-cysteine accessibility method (SCAM) (Akabas et al., 1992; Karlin and Akabas, 1998; Javitch et al., 2001) to map the surface of the binding-site crevice in the dopamine D_2 receptor (Javitch et al., 1994, 1995a,b, 1998, 1999, 2000; Fu et al., 1996; L. S., M. M. Simpson, J. A. B., and J. A. J., in preparation), a member of the class A receptor family. In this method, each of the residues in the seven TMs is mutated to Cys, one at a time, and the mutant receptors are expressed in heterologous cells. After confirming that the receptor expresses and binds ligand in a near-normal manner, we assess the water-accessibility of the engineered Cys by determining the effects of treatment with a series of charged sulfhydryl reagents. These reagents, derivatives of methanethiosulfonate (MTS), are more than a billion times more reactive with the thiolate anion than with the thiol (Roberts et al., 1986) and only water-accessible Cys are expected to be significantly ionized. Because of this and because the reagents are charged, we expect that water-accessible Cys residues will be vastly more reactive with the MTS reagents than will Cys facing lipid or facing the tightly packed protein interior. We infer that a wild-type residue is on the water-accessible surface if reaction of a MTS reagent with the corresponding engineered Cys irreversibly alters radioligand binding. We further infer that the residue faces the binding-site crevice if ligand is able to retard the reaction of the MTS reagents with the engineered Cys.

The results of our SCAM studies of the dopamine D_2 re-

TABLE 1

Rhodopsin helix-helix interactions found experimentally.

Cβ-Cβ is the distance between the Cβ of two residues in the bovine rhodopsin structure. Receptor names are abbreviated according to their SWISS-PROT Annotated Protein Sequence Database entry names: http://www.expasy.ch/cgi-bin/lists?7trmrlist.txt

Residue Indices		Experimental Methods						Residues/Mutations		Cβ-Cβ	References
		C	R	Z	E	L	F				
										Å	
1.60	7.63	+			+			H65C	C316	5.3	Yang et al., 1996; Struthers et al., 2000
2.57	7.43		+					G90D	K296	8.3[a]	Oprian, 1992; Rao et al., 1994
3.28	7.43					+		E113	K296	10.1	Oprian, 1992; Rao et al., 1994
3.36	5.22	+						C110	C187	12.9	Struthers et al., 2000
3.36	6.44		+					G121L	F261A	9.0	Han et al., 1996; Lin et al., 2000
3.37	5.46						+	E122	H211	6.1	Beck et al., 1998
3.51	5.57	+						Y136C	C222	5.1	Yu and Oprian, 1999
3.51	5.60	+						Y136C	C225	6.0	Yu and Oprian, 1999
3.53	6.34			+				V138H	T251H	8.3	Sheikh et al., 1996
3.54	5.60			+				V139C	Q225C	8.6	Yu and Oprian, 1999
3.54	6.30	+						V139C	E247C	6.3	Farrens et al., 1996
3.54	6.31	+			+			V139C	K248C	8.2	Farrens et al., 1996
3.54	6.32	+			+			V139C	E249C	11.8	Farrens et al., 1996
3.54	6.33	+			+			V139C	V250C	8.9	Farrens et al., 1996
3.54	6.34	+			+			V139C	T251C	5.7	Farrens et al., 1996
3.54	6.35				+			V139C	R252C	10.8	Farrens et al., 1996
3.55	5.57	+						C140	C222	8.3	Farrens et al., 1996; Yu and Oprian, 1999
3.55	5.60	+						C140	Q225C	4.9	Yu and Oprian, 1999; Struthers et al., 2000
3.55	7.63	+						C140	C316	28.5[a]	Yu et al., 1999
5.33	6.59	+						T198C	F276C	14.5	Struthers et al., 1999
5.35	6.59	+						N200C	F276C	9.0	Struthers et al., 1999
5.39	6.59	+						V204C	F276C	5.1	Struthers et al., 1999, 2000

C, Cys-Cys crosslinking; R, double revertant mutations; Z, Zinc-His binding; E, spin-labeling; L, ligand related; F, Fourier-transform infrared difference spectroscopy.
[a] Present only in the active state.

TABLE 2

Other GPCR helix-helix interactions found experimentally.

Cβ-Cβ is the distance between the Cβ of two residues in bovine rhodopsin structure. Receptor names are abbreviated according to their SWISS-PROT Annotated Protein Sequence Database entry names: http://www.expasy.ch/cgi-bin/lists?7tmrlist.txt

Residue Indices	Receptors	Experimental Methods			Residues/Mutations	Cβ-Cβ	References
		C	R	Z			
1.39 7.36	ACM2-ACM5		+		T37A H423T	11.8	Liu et al., 1995
2.50 7.49	GRHR		+		N87D D318N	7.0	Zhou et al., 1994
2.50 7.49	5H2A		+		D120N N376D	7.0	Sealfon et al., 1995
2.64 3.28	NK1R			+	Y92H H108	6.6	Elling and Schwartz, 1996
3.29 5.35	NK1R			+	N109H E193H	14.0	Elling and Schwartz, 1996
3.32 7.39	B2AR			+	D113H N312C	15.5[a]	Elling et al., 1999
3.43 6.44	ACM1			+	L116H F374H	6.3	Lu and Hulme, 2000
3.43 7.49	ACM1			+	L116H N414H	10.1	Lu and Hulme, 2000
3.53 6.30	B2AR			+	A134H E268H	6.1	Sheikh et al., 1999
3.53 6.31	B2AR			+	A134H H269	10.7	Sheikh et al., 1999
3.53 6.34	B2AR			+	A134H L272H	8.3	Sheikh et al., 1999
3.54 6.29	ACM2	+			I169C K484C	11.5	Zeng et al., 1999
3.54 6.30	ACM3	+			I169C E485C	6.3	Zeng et al., 1999
3.54 6.31	ACM3	+			I169C K486C	8.2	Zeng et al., 1999
3.54 6.32	ACM3	+			I169C K487C	11.8	Zeng et al., 1999
3.54 6.33	ACM3	+			I169C A488C	8.9	Zeng et al., 1999
3.54 6.34	ACM3	+			I169C A489C	5.7	Zeng et al., 1999
3.54 6.35	ACM3	+			I169C Q490C	10.8	Zeng et al., 1999
3.54 6.36	ACM3	+			I169C T491C	12.4	Zeng et al., 1999
5.35 6.59	NK1R			+	E193H Y272H	9.0	Elling et al., 1995
5.39 6.55	NK1R			+	H197 F268H	8.6	Elling et al., 1995
5.39 6.56	NK1R			+	H197 L269H	8.5	Elling et al., 1995
5.39 6.59	NK1R			+	H197 Y272H	5.1	Elling et al., 1995
6.44 7.49	ACM1			+	F374H N414H	9.0	Lu and Hulme, 2000
TM1/TM2 7.39	B2AR-A2AA		+		N312F		Mizobe et al., 1996
TM3/TM6 7.38	B2AR-A2AA		+		L311F		Mizobe et al., 1996

C, Cys-Cys crosslinking; R, double revertant mutations; Z, Zinc-His binding; E, spin-labeling; L, ligand related; F, Fourier-transform infrared difference spectroscopy.
[a] Present only in the active state.

ceptor are shown in Figs. 2B and 3B and in further detail below in our discussion of each TM. In general, there is remarkably good agreement between the residues found to be accessible in the D_2 receptor and the residues that face the protein-protein interface in the rhodopsin structure (Fig. 2B). Indeed, of the residues that have been inferred to face the binding-site crevice, 79% have low SASA (<10%). The patches of accessible residues on helix faces are generally a bit narrower than those predicted to face the protein-protein interface. This finding is consistent with the notion that at the extreme margins of the protein-protein interface the helices may be more tightly packed than at the surface of the binding-site crevice. At the extracellular end of the TMs, the SCAM results in general give a broader pattern of accessibility than predicted, consistent with access from the extracellular milieu to an entire turn of helix, with the greater water-accessibility of residues in the phospholipid headgroup region (see above) and/or with dynamic changes of the structure in these regions broadening the experimentally determined accessibility compared with either the predictions or the static crystal structure of the inactive state of rhodopsin. We address below some of the detailed results of SCAM of the D_2 receptor, but the overall results are presented in Fig. 3B, which shows an extracellular view of the backbone of rhodopsin. The Cβ and backbone ribbon of the residues for which the aligned positions in the D_2 receptor are accessible are shown in yellow (accessible and protected) and in orange (accessible but not protected, or protection could not be tested reliably because of small effect sizes).

Tertiary Structure Interactions

Various experimental methods have been used to explore helix-helix interactions in rhodopsin and in rhodopsin-like receptors. These include the creation of metal binding sites (Elling et al., 1997), disulfide cross-linking between adjacent helices (Farrens et al., 1996), and the discovery of double revertant mutations in which a second-site mutation restores function lost by a first mutation (Zhou et al., 1994; Sealfon et al., 1995). The findings from these studies are summarized in Tables 1 and 2, which show the actual distances between the aligned residues in the three-dimensional structure of rhodopsin. In Fig. 4 these interactions are shown in an extracellular view of ideal α-helical wheels positioned according to the rhodopsin projection structure. The vast majority of these interactions are consistent with the high-resolution structure of rhodopsin. Certain interactions that appear to be inconsistent with the rhodopsin structure, such as 2.50 to 7.49, are in fact compatible, because of the presence of bends and twists in the helices that cannot be conveyed in ideal α-helical wheels. The compatibility of tertiary structure distances among the aligned positions of different GPCRs suggests the presence of significant similarity in the overall helical packing, even in regions in which rhodopsin contains local distortions in helical structure (see below). Other experimentally determined interactions are not consistent with the rhodopsin structure, and these require that the structure be dynamic. Examples of these include the stretch of residues 6.30 to 6.34 at the cytoplasmic end of TM6 that were all cross-linked to 3.54 at the cytoplasmic end of TM3. In this case, both the cross-linking data and the high-resolution structure come from bovine rhodopsin, so the differences are probably explained by protein dynamics or conformational changes in the receptor. In other cases, such as 3.32 to 7.39 in the β_2 adrenergic receptor and 3.55 to 7.63 in rhodopsin, the contacts were inferred to be present in the active state; not

surprisingly, these are incompatible with the inactive rhodopsin structure and require a significant conformational change.

To address in more detail the similarities and differences between rhodopsin and other class A receptors, we need to focus on those domains that show at least some significant sequence homology and could support similarities at the structural level. The extracellular and cytoplasmic domains of GPCRs are widely divergent, thus precluding any direct comparison between rhodopsin and other GPCRs. We have therefore focused our analysis on the transmembrane domain to explore the extent to which the recently available structure of rhodopsin is a feasible structural template for other class A receptors, with special emphasis on amine GPCRs. We will review below each TM and examine the conserved and nonconserved motifs and how these might be expected to affect the resulting structure. The accessibility pattern determined in our SCAM studies on the D_2 receptor will be used to guide this analysis. In such an analysis, special attention must be paid to potential deviations from ideal α-helicity that result from residues known to produce kinks and bends. Because their side chains are covalently bonded to the backbone, prolines produce kinks in α-helices caused by steric clash of the pyrrolidine ring with the backbone and to loss of the hydrogen bond (H-bond) between the amide nitrogen and the carbonyl at the (i-4) position (Barlow and Thornton, 1988; Sankararamakrishnan and Vishveshwara, 1992; Sansom and Weinstein, 2000). Glycines are also commonly found at kinks in α-helices, presumably because of the flexibility they induce (Kumar and Bansal, 1998). In addition, serine, threonine, and cysteine can significantly bend and twist α-helices because of their ability to hydrogen bond back to the backbone carbonyl of the preceding turn (Gray and Matthews, 1984; Ballesteros et al., 2000).

TM1

Most class A receptors do not have a Pro at position 1.48, whereas Pro1.48 is present in most vertebrate opsins. The proline kink in TM1 of bovine rhodopsin bends TM1 inwards, toward the helix bundle. The absence of such a kink in other GPCRs would orient an ideal α-helix more outward, away from the bundle and toward lipid and toward TM7 (Fig. 5A). The extracellular portion of TM1 in amine receptors is less conserved than the aligned region in the opsin family. This is consistent with the relative lack of key contacts, as well as with the generally minimal effect of mutations in this region and with the SCAM analysis of the dopamine D_2 receptor in which the extracellular part of TM1 does not seem to contribute to the surface of the binding-site crevice (L. S., M. M. Simpson, J. A. B., and J. A. J., in preparation). Thus, it is possible that TM1 has a more outward orientation in the amine receptors, which lack Pro1.48 (Fig. 5A). There may be changes in the relative disposition of TM2 and TM7 to adjust for the potentially altered packing of TM1, but it is also possible that bulkier side chains may serve to fill the potential space. The large number of bulky side chains of the D_2 receptor in the TM2-TM3-TM7 aromatic microdomain may be an example of such an adaptation (Javitch et al., 1999; Simpson et al., 1999).

Recent work, however, showed that removal of a conserved Pro from a kinked α-helix in heat shock transcription factor did not prevent the formation of the kink (Hardy et al., 2000). Most opsins have a Pro at 1.48, but those that do not have a preponderance of Thr and Gly at the 1.49 position. The presence of these residues is also associated with bent helices (Kumar and Bansal, 1998; Ballesteros et al., 2000) and either might substitute for Pro to maintain a kink in TM1. Likewise, Gly1.49 is very highly conserved in amine receptors, which lack a Pro at 1.48, and the increased flexibility induced by this Gly might also support a kink in TM1, even without the Pro.

TM2

Bovine rhodopsin has three Thr (2.59–2.61) in TM2, but other rhodopsin sequences contain Pro at 2.58, 2.59, and/or 2.60, either individually or in combination. Although TM2 of bovine rhodopsin has no Pro, it does contain a significant kink within the 2.56–2.60 helix turn defined by Gly-Gly-X-Thr-Thr. In this motif, the Thr's side chains hydrogen bond to the carbonyls at the (i-4) positions, stabilizing a bent conformation (Fig. 5B). The Gly residues probably add flexibility, further facilitating this bent structure. The D_2 receptor and many other GPCRs contain Pro2.59, so we expect a bend at the 2.55 to 2.59 helix turn formed by the Pro-kink, at a similar position as the bend in rhodopsin. Pro-kinks are flexible and can adopt different extents of bending. We have illustrated this flexibility and the conformational space that can be explored by the Pro-kinked helix by performing a molecular dynamics simulation of an α-helix with a Pro (Fig. 5C). Different GPCRs have a single Pro at 2.58, 2.59, or 2.60, and each one of these positions would be expected to orient the bend differently (Fig. 5C). If we choose from the simulations the Pro-kink conformation with the lowest RMSD compared with rhodopsin (RMSD = 2.0 Å), then the resulting D_2 receptor Pro-kinked structure has a backbone orientation similar to that of rhodopsin and is consistent with the SCAM data (Fig. 5D). Thus, the extent of bend could be quite similar in related GPCRs, even to the point that it is achieved in TM2 with a Gly-Gly-X-Thr-Thr motif as well as with Pro, an example of the sort of structural mimicry we propose. Nonetheless, the fact that the Pro can be in different positions suggests that this may be a source of considerable structural diversity in other class A receptors. An example involving a Thr-X-Pro motif in TM2 of the CCR5 receptor has been proposed recently (Govaerts et al., 2001).

TM3

Compared with TM2, TM3 of bovine rhodopsin contains more subtle bends that result from the presence of Ser, Thr, and Cys. As described above, these residues can hydrogen bond to the backbone and thereby bend and twist helices (Gray and Matthews, 1984; Ballesteros et al., 2000). The resulting bends are likely to be somewhat different in related GPCRs because of different positioning of Cys/Ser/Thr. Interestingly, when TM3 of the D_2 receptor is modeled as an ideal α-helix and superimposed on the conserved cytoplasmic region of TM3 in rhodopsin, the ideal helix clashes sterically with TM4 (white ribbon in Fig. 5E). Although the bends in the D_2 receptor may not be extreme enough to be detected by SCAM as a gross alteration in the pattern of accessibility in TM3, such bending may nonetheless alter the position of TM3 relative to TM4 (see below). In Fig. 5E, we have illustrated the wide range of bending and twisting that can result from the presence of Cys/Ser/Thr residues in the D_2 receptor.

It has been shown recently that different rotamer conformations of these side chains differentially alter the Φ and Ψ dihedral angles of the helix backbone, resulting in different local bends (Gray and Matthews, 1984; Ballesteros et al., 2000). For every combination of rotamer conformations of Cys/Ser/Thr residues in TM3 of the D_2 receptor, we modeled the corresponding average deviation in Φ and Ψ angles starting from the ideal TM3 helix backbone. The result is a set of alternative possible TM3 conformations for the D_2 receptor, shown in Fig. 5E superimposed on TM3 of rhodopsin, which is also bent because of the presence of these residues at different positions in rhodopsin. Different TM3 conformations might represent different functional states of the same receptor, such as liganded versus unliganded or active versus inactive. Nonetheless, a conformation can be chosen for the D_2 receptor that closely mimics rhodopsin (RMSD = 2.0 Å) (Fig. 5F), suggesting that particular sets of interactions of otherwise divergent positioning of Cys/Ser/Thr residues in TM3 of different receptors may lead to similar folds of the TM3 segment.

We quantified in each TM of amine receptors the number of positions at which either a Ser, a Thr, or a Cys is present in more than 50% of all amine GPCRs. TM3 contains seven of these conserved Cys/Ser/Thr positions, whereas TM5 contains 4, and the other TMs contain one to three. Thus, given the large number of Cys/Ser/Thr, the high degree of conformational heterogeneity and/or flexibility proposed above for TM3 of the D_2 receptor may be shared by TM3 of other amine GPCRs. The fact that five of these positions are incompletely conserved as Cys/Ser/Thr provides for potential divergence in the conformation of TM3 in different amine GPCRs. Therefore, the set of different bends of TM3 in the D_2 receptor illustrates not only the potential conformational variability within a single GPCR, but also the extent of conformational variability possible among different GPCRs in TM3 given the different patterns, yet prevalent presence of Cys/Ser/Thr in this TM.

TM4

TM4 is the shortest membrane-spanning helix in rhodopsin, and sequence alignments indicate that it probably is also short in most other GPCRs (Ballesteros and Weinstein, 1995). The TM4 α-helix in rhodopsin is disrupted by a Pro-Pro motif at position 4.59, followed by a short helical turn. The presence of Pro-Pro, or Pro-X-Pro motifs around 4.59 is common to many class A GPCRs, whereas some GPCRs, such as D_2 or β_2 adrenergic receptors, have only a single Pro at 4.59 (Javitch et al., 2000). The lack of a significant conservation pattern in GPCRs beyond this motif suggests that the structure beyond these Pro motifs, in particular the short helical turn, might not be conserved in other GPCRs. Our accessibility studies in the D_2 receptor, however, were consistent with the presence of a short helical turn for the equivalent residues in rhodopsin (Javitch et al., 2000), suggesting that such a motif might be conserved despite the absence of any recognizable sequence conservation. Given the inherent flexibility of all three motifs (Pro-kink, Pro-Pro, or Pro-X-Pro), the overall orientation of a short helical turn ending the TM4 helix may either be different in other GPCRs or, alternatively, may share a similar fold.

Trp4.50 is highly conserved, and thus we had predicted that it would face the binding-site crevice. Moreover, we found that Cys substituted for this Trp, as well as for Phe4.54 in the D_2 receptor, were accessible to MTS reagents and protected by an antagonist (Javitch et al., 2000). Surprisingly, in the rhodopsin structure, a significant part of the aligned Trp and of Leu165$^{4.54}$ is exposed to lipid at the margin of TM3 and TM2. As can be seen in Fig. 6A, the superimposition of the SCAM results on TM4 of rhodopsin seems to place the accessible face rotated approximately 90° too far counter-clockwise (seen extracellularly) given the relative position of TM3. The explanation for this apparent anomaly is not clear and may involve alterations in the packing and relative disposition of the TMs. Nonetheless, it would be surprising for the structures to be dramatically different in this region given the extremely high conservation of Trp4.50. The lipid exposure of the conserved Trp4.50 may be related to the known requirement of rhodopsin activation for polyunsaturated lipids (Gibson and Brown, 1993), which would interact favorably with Trp4.50. Alternatively, 4.50 and 4.54 may face outward to participate in yet unknown protein-protein interactions within the membrane, such as receptor dimerization, which could conceivably explain the observed accessibility to charged MTS reagents.

TM5

TM5 in Class A receptors is predicted to be a Pro-kinked α-helix, because of the highly conserved Pro residue at position 5.50. However, relative to standard Pro-kink conformations, the rhodopsin structure shows a very unusual kink, characterized by a bulge, or local unwinding, around residue His211$^{5.46}$. This His residue probably participates in an ionic interaction or a strong H-bond with the negatively charged Glu122$^{3.37}$ in TM3 (Beck et al., 1998), and such an interaction (Fig. 6B) in the transmembrane domain may be responsible for perturbing the Pro-kink backbone conformation in the unusual manner observed in the crystal structure.

The pair His211$^{5.46}$-Glu122$^{3.37}$ is not conserved in other GPCRs. The question is thus whether other GPCRs also contain such an unusual bulge in TM5 or form a more standard Pro-kink conformation. To address this question, we generated a standard Pro-kinked α-helix, and we also created a set of 100 representative structures from molecular dynamics simulations of the Pro-kinked TM5 of the D_2 receptor; these were superimposed on the relatively conserved cytoplasmic segment (5.51–5.58) of rhodopsin. The representative Pro-kinked structure with the best fit to the extracellular portion of TM5 of rhodopsin had an RMSD of 2.6 Å. Nonetheless, when superimposed in this manner, neither the ideal Pro-kink, nor any of the 100 Pro conformations, positioned 5.42 facing the binding-site crevice (Fig. 6C). This is inconsistent with mutagenesis studies of residue 5.42 in various amine GPCRs, which suggested the presence of a direct ligand-receptor interaction at this locus, such as the proposed interaction with the *meta*-OH of catecholamines (Liapakis et al., 2000) and with SCAM data on the D_2 receptor showing accessibility and protection of Cys substituted at position 5.42. Therefore, although we might have expected a more standard Pro-kink conformation for TM5 in the D_2 and other catecholamine receptors compared with rhodopsin, these structures cannot satisfy established ligand-receptor contacts. In contrast, the face twist accomplished by the bulge in rhodopsin TM5 reorients 5.42 and 5.43 toward the binding-site crevice (Fig. 6C). This suggests that the structure in

these other GPCRs may be similar to that in rhodopsin, despite the absence of the pair His5.46-Glu3.37.

What molecular mechanisms might be responsible for reorienting the extracellular portion of TM5 (5.37–5.46) in the absence of the His5.46-Glu3.37 bond present in rhodopsin? This portion of TM5 in amine GPCRs such as the D_2 receptor contains conserved Cys/Ser/Thr residues at positions 5.42, 5.43, and 5.46, all on the same face of TM5 proposed to interact directly with catecholamine hydroxyls. These Cys/Ser/Thr residues, as mentioned before, can hydrogen bond to the backbone carbonyls of the preceding turn, thereby bending and twisting the helix (Gray and Matthews, 1984; Ballesteros et al., 2000). We found in molecular dynamics simulations that the local helix distortions created by Ser residues at 5.42, 5.43, and 5.46, in conjunction with the Pro-kink created by Pro5.50, are able to increase the range of possible structures and accomplish the face shift necessary to satisfy the SCAM and mutagenesis data by producing a bulge rather similar to that seen in rhodopsin (Fig. 6D; the "best" RMSD is only 1.2 Å). This demonstrates that the specific and unusual features of the rhodopsin structure, such as the bulge in TM5, might be accomplished through structural mimicry in which different molecular mechanisms or interactions can produce similar structures in different receptors.

The high degree of conformational heterogeneity and/or flexibility observed in the simulations for the top of TM5 of the D_2 receptor, enabled by the Pro-kink and the multiple interactions of the Ser at 5.42, 5.43, and 5.46 with the backbone, might also help to explain the broad pattern of accessibility observed by SCAM in this region of TM5 (Javitch et al., 1995a). However, the equivalent SCAM studies on TM5 performed on the β_2 receptor found a narrower face of TM5 accessible to the binding-site crevice (G. Liapakis, L. S., D. Fu, and J. A. J., in preparation). This suggests that the extracellular region of TM5 preceding Pro5.50 may behave differently in different receptors, for instance being more flexible in the D_2 receptor than in the β_2 receptor. The significant range of conformational heterogeneity and/or flexibility observed at the top of TM5 within the D_2 receptor may actually be related to different functional states of the receptor, such as inactive versus active conformations. Furthermore, because different amine GPCRs show different patterns of Cys/Ser/Thr in this region, and many other GPCRs lack these Cys/Ser/Thr altogether, we might expect some degree of structural divergence for the extracellular portion of TM5 in different GPCRs.

TM6

TM6 in rhodopsin is a more typical α-helix with a pronounced kink around the highly conserved Pro6.50. For other GPCRs, this conserved Pro residue is also expected to result in a Pro-kink, which could adapt a number of conformations as illustrated in Fig. 5C for TM2. Spin-labeling studies in rhodopsin were consistent with a displacement of the cytoplasmic side of TM6 away from TM3 upon rhodopsin activation (Farrens et al., 1996), and Cys crosslinking of residues in these regions blocked receptor activation (Sheikh et al., 1996). Although this movement has been interpreted as a rigid body movement of the entire TM6 helix upon activation (Farrens et al., 1996), we have proposed that the extent of bending of the Pro-kink is associated with receptor activation (Jensen et al., 2000; Sansom and Weinstein, 2000; Ballesteros et al., 2001; Visiers et al., 2001). The role of the conserved Pro-kink in TM6 as a flexible hinge underpinning this conformational change has been recently supported by mutagenesis of residues within the Pro-kink of the β_2 adrenergic receptor combined with simulations, which suggest that a straightening of TM6 about the kink and a resulting movement of the cytoplasmic portion of TM6 away from TM3 is associated with receptor activation (G. Liapakis, L. S., R. Xu, F. Guarnieri, J. A. B., and J. A. J., in preparation). There is, therefore, an apparent conservation of the mechanism of

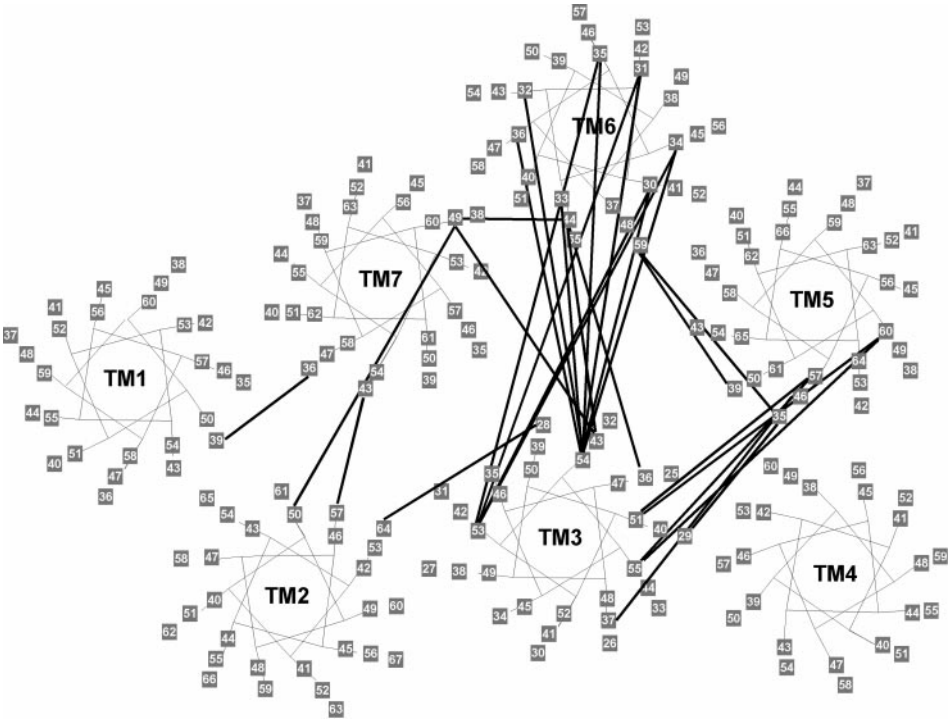

Fig. 4. Helical wheel representation assuming ideal α-helices of the experimentally derived TM-TM interactions. The detailed interactions are listed in Tables 1 and 2.

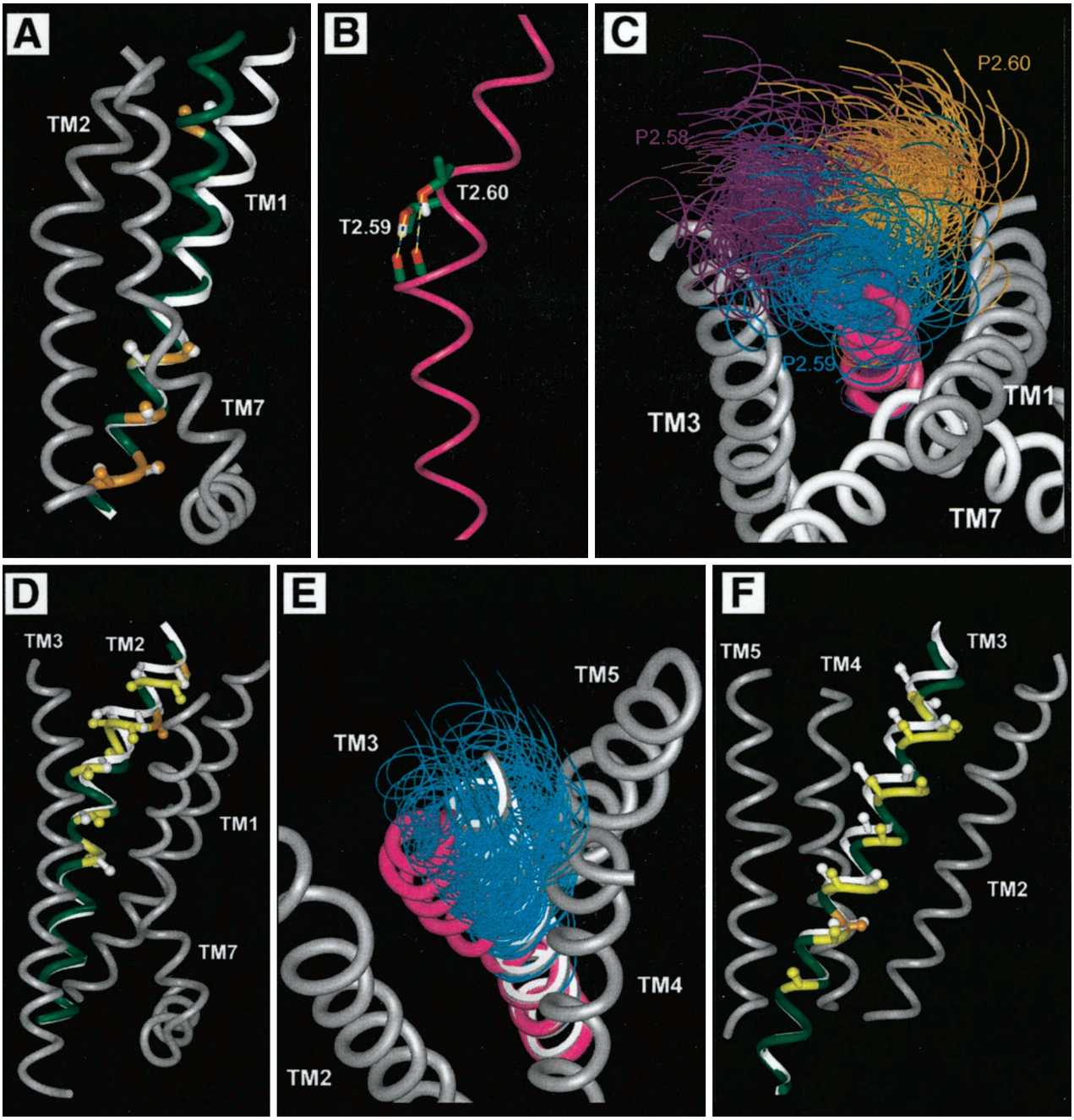

Fig. 5. TM1–3. A, three-dimensional molecular representations of TM1, in the context of TM2 and TM7, showing the Cα traces from the high-resolution structure of bovine rhodopsin. The top of the panel shows the extracellular end and the bottom of the panel the intracellular end of the TMs. The Cα ribbons of TM2 and TM7 are shown in gray; for TM1, the Cβs of the rhodopsin residues aligned with the accessible D_2 receptor residues are shown in orange. The protected 1.50 is shown in yellow. The remaining residues in TM1 are shown in green without Cβ. To simulate the absence of Pro1.48 in the D_2 receptor, an ideal α-helix (white ribbon) is superimposed on TM1 from 1.49 to 1.59. B, three-dimensional molecular representation of the Gly-Gly-X-Thr-Thr motif bending the α-helix in TM2 of rhodopsin. The top of the panel shows the extracellular end and the bottom of the panel the intracellular end of the TM. The Cα ribbon of TM2 is shown in pink. The carboxyl atoms of Phe88$^{2.55}$, Gly89$^{2.56}$, and the heavy atoms of side chains with the hydrogen of the hydroxyl groups of Thr92$^{2.59}$, Thr93$^{2.60}$ are shown. The H-bonds between Thr92$^{2.59}$ and Phe88$^{2.55}$ and between Thr93$^{2.60}$ and Gly89$^{2.56}$ are shown by dashed yellow lines. C, three-dimensional molecular representation viewed extracellularly of TM2, in the context of TM1, TM3, and TM7, showing the Cα traces from the high-resolution structure of bovine rhodopsin with TM2 in pink; TM1 and TM3 are shown in gray; TM7 is shown in white. The 100 simulated α-helices from molecular dynamic simulations (see *Materials and Methods*) are superimposed from 2 to 18 (P2.58 cluster shown in deep purple), 1 to 17 (P2.59, blue), and 1 to 16 (P2.60, orange) onto the corresponding parts of TM2 (2.38 to 2.54). In D, the Cα ribbons of TM1, TM3 and TM7 are shown in gray; for TM2, the Cβs of the rhodopsin residues aligned with the accessible D_2 receptor residues are shown in orange or in yellow for those that were protected. The remaining residues in TM2 are shown in green without Cβ. The Cα ribbon of the structure from the P2.59 cluster in A with the smallest RMSD compared with rhodopsin is shown with the Cβs of aligned accessible residues in white. E, three-dimensional molecular representation viewed extracellularly of TM3, in the context of TM2, TM4, and TM5, showing the Cα traces from the high-resolution structure of bovine rhodopsin. The Cα ribbon of TM3 is shown in pink; TM2, TM4, and TM5 are shown in gray. An ideal α-helix (white ribbon) is superimposed on TM3 from 3.48 to 3.54. The 54 simulated α-helices for TM3 (see *Materials and Methods*) are superimposed (thin blue ribbons) on TM3 from 3.48 to 3.54. In F, the top shows the extracellular end and the bottom the intracellular end of the TMs. The Cα ribbons of TM2, TM4 and TM5 are shown in gray; for TM3, the Cβs of the rhodopsin residue aligned with the accessible D_2 receptor residue is shown in orange. The protected residues are shown in yellow. The remaining residues in TM3 are shown in green without the Cβ. The Cα ribbon of the structure from E with the smallest RMSD compared with rhodopsin is shown with the Cβs of aligned accessible residues in white.

receptor activation across different receptors, involving a movement of the cytoplasmic side of TM6 away from TM3, facilitated by the conserved Pro-kink at position 6.50 acting as a flexible hinge. Therefore, we would expect that other GPCRs also share a highly kinked conformation of the Pro-kink in TM6 in the inactive conformation, which becomes less kinked upon receptor activation.

There is very good agreement between the empirically determined water-accessible face of TM6 in the D_2 receptor, and the orientation of the aligned residues in rhodopsin (Fig. 6E), consistent with our interpretation of the presence of a Pro-kink in the D_2 receptor (Javitch et al., 1998). Also corroborated in the rhodopsin structure is the orientation of the cluster of aromatic residues in the D_2 receptor identified by SCAM and mutagenesis as facing the binding-site crevice (Javitch et al., 1998), where these residues form a critical interaction with the aromatic ring of catecholamine ligands. The interaction of the aromatic residues in this cluster with ligands in the binding-site crevice was originally proposed in the β_2 adrenergic (Dixon et al., 1988) and 5HT2a receptors (Choudhary et al., 1995; Roth et al., 1997) and is likely to be a feature shared by other GPCRs as well.

TM7

TM7 of rhodopsin and of other class A receptors contains the highly conserved Asn-Pro motif at 7.49 and 7.50, which is expected to kink the TM7 helix. Curiously, TM7 of rhodopsin has a very unusual kinked conformation around Pro7.50, with a turn of tightly wrapped 3_{10} helix at position 7.43–7.46 (Fig. 6F). An unusual conformation around the Asn-Pro motif in TM7 had been suggested based on photolabeling studies of rhodopsin (Findlay et al., 1984). This unusual 3_{10} helix conformation may be related to or stabilized by the covalent attachment of retinal to Lys296$^{7.43}$ in rhodopsin (Fig. 6F). The question thus arises whether the structure of TM7 in other GPCRs may contain a similar motif in TM7, in the absence of the Lys7.43-retinal attachment interaction. The first inference that the Asn-Pro motif in TM7 of other GPCRs may be specially distorted arose from double-revertant mutant studies performed in the 5HT2a and GnRH receptors between Asp2.50 in TM2 and Asn7.49 in TM7 (Zhou et al., 1994; Sealfon et al., 1995), which suggested a direct interaction between these residues that was inconsistent with a standard Pro-kink in TM7. The pattern of accessibility of TM7 determined by SCAM was also more consistent with a highly twisted α-helix around the Asn-Pro motif but not with a standard α-helix (Fu et al., 1996). In particular, residue Ser7.46 in TM7 of the D_2 receptor was not accessible, yet surrounded by accessible residues in a standard α-helical conformation (Fig. 2B).

Gouldson et al. (1997) predicted the presence of 3_{10} helix in TM7 to explain the D_2 receptor SCAM and other mutagenesis data, but they placed the 3_{10} helix one turn below its position in the rhodopsin structure. The SCAM data in the D_2 receptor is remarkably consistent with the rhodopsin TM7 conformation (Fig. 6G), whereas it is less compatible with a standard Pro-kink or any of the simulated Pro-kinks (data not shown). Indeed, the apparent lack of accessibility of Ser7.46, which was difficult to explain even with the extreme bend and twist we previously hypothesized to explain the TM7 SCAM data (Fu et al., 1996) is explained in the rhodopsin structure in which the 7.46 side chain is completely surrounded by side chains from TM1 and TM2 (Fig. 6G). Furthermore, residues Asp2.50 from TM2 and Asn7.49 from TM7 are nearby in the rhodopsin structure, potentially interacting through a water molecule, consistent with the predictions based on the double revertant mutant studies. We suspect therefore that the structure of TM7 in the other class A receptors that lack the Lys296$^{7.43}$-retinal is similar to that of rhodopsin, although different molecular interactions may be responsible for stabilizing a similar motif in different GPCRs, another example of structural mimicry.

The cytoplasmic extension of TM7 has been proposed to form an α-helix based on NMR studies of a peptide of this region (Albert and Yeagle, 2000), and secondary structure predictions also suggested that this region was α-helical (Ballesteros and Weinstein, 1995; Visiers et al., 2001). Indeed, this region is an α-helix in rhodopsin, and it has been termed H8. The linker between TM7 and H8 is highly divergent among GPCRs, with several insertions, deletions, or nonconserved Pro residues present, suggesting a lack of conserved secondary structure in this region. Nonetheless, the linker in rhodopsin was inferred to be α-helical based on spin-labeling experiments (Altenbach et al., 1999a; Fig. 2A), suggesting that the structure of this region may be dynamic. Although the structure of the linker is unclear, it is likely that the H8 region also forms an α-helix in other receptors. Several residues that face into the rhodopsin core are highly conserved, including Phe313$^{7.60}$, which is in close contact with the cytoplasmic portion of TM1 (Thr58$^{1.53}$, Val61$^{1.56}$, and Thr62$^{1.57}$). Residues 1.53 and 1.57 in TM1 are highly conserved as β-branched residues among amine GPCRs, and in the D_2 receptor, the residues at positions 1.53, 1.56, and 1.57 were found to be accessible by SCAM (L. S., M. M. Simpson, J. A. B., and J. A. J., in preparation). The high conservation observed for the residues forming the H8-TM1 interface suggests that a similar packing arrangement may be present for H8 in other GPCRs. In addition, the residues facing solvent are conserved in their α-helical pattern of Arg/Lys. These basic residues have been proposed to face the phospholipid headgroups (Fig. 3A), and are present on only one side of H8 (every three to four residues), suggesting that the helical conformation of H8 is maintained in other GPCRs. (An exception to this is the GnRH receptor, which seems to lack H8.) Although H8 has been proposed to play a role in activation, the details of such a role remain uncertain. Crosslinking data in rhodopsin, however, suggest that the conformational movement of H8 with activation is quite large (Yang et al., 1996; Yu et al., 1999; Table 1).

In summary, although the figures shown for the TMs of the D_2 receptor are illustrations showing possible conformations, based on the SCAM and mutagenesis data, it appears possible that the helical packing and extent of bends and twists is quite similar in rhodopsin and in the D_2 receptor and other amine GPCRs. We hypothesize that through structural mimicry these related GPCRs have evolved different microdomains (such as Thr-Thr versus Pro) to maintain their similar overall structure, while accommodating other changes necessary to make them selective for their ligands, such as the flexibility inherent in multiple Pro-kinks and Cys/Ser/Thr motifs. At the same time, divergence in some of these features, such as the position of the Pro in TM2 or of the Cys/Ser/Thr in TM3, is a potential mechanism for structural diversity in other class A receptors, and flexibility about the

Pro-kinks or other induced bends in a given receptor is also a potential mechanism for conformational changes related to function.

The Binding Site

The SASA analysis of the high-resolution structure of rhodopsin described above was used to quantify the lipid-accessible surface of the protein (Fig. 2). We have also performed such an analysis in the presence and absence of retinal. The difference between these two calculated surfaces represents the surface of the binding-site crevice that is protected from water by retinal. The residues identified by this analysis in the TMs (see Table 3) are highlighted in Fig. 7A, in which the retinal is shown within the binding-site crevice formed by the retinal-"protected" residues. The positions of these residues are remarkably consistent with those of previously identified ligand-receptor contact sites for amine GPCRs (Table 3), as well as with our SCAM studies of the dopamine D_2 receptor. Figure 7B illustrates this agreement with the backbone of the rhodopsin structure and the side chains of the β_2 adrenergic receptor that have been shown to interact directly with catecholamine ligands. These residues include Asp113$^{3.32}$, which interacts with the protonated amine of biogenic amines; Ser203$^{5.42}$, Ser204$^{5.43}$, and Ser207$^{5.46}$, which interact with the *meta*-OH and *para*-OH of catecholamines; Asn293$^{6.55}$, which interacts with the β-OH of epinephrine; and Phe208$^{5.47}$ and Trp286$^{6.48}$, Phe289$^{6.51}$, and Phe290$^{6.52}$; which form a cluster of aromatic residues in TM5 and TM6 that interact with the aromatic ring of ligands. Even without modification of the rhodopsin backbone, it is clear that epinephrine fits remarkably well within the binding site formed by these critical residues.

In Fig. 7C, we illustrate *p*-(Bromoacetamido)benzyl-1-[^{125}I]iodocarazolol (IpBABC), an affinity label derivative of pindodol, docked within the TMs of the rhodopsin structure with all the residues from Table 3 mutated to the aligned β_2 adrenergic receptor residues. IpBABC is shown covalently attached to His93$^{2.64}$ in TM2, the likely site of covalent reaction (Dohlman et al., 1988; Javitch et al., 1999). Again, the ligand is bound essentially to an overlapping set of the residues that contact retinal in rhodopsin. It is important to note that although some of the residues in the binding-site crevice of these receptors are conserved, most are not. Thus, these residues have apparently evolved to impart specificity within a certain receptor. Consequently, what is "conserved" among these receptors is the *positions* of the residues involved in ligand binding and thus the particular surface that serves the role of ligand binding.

Although the location of the binding site seems to be conserved in rhodopsin and amine receptors, this need not be the case for all class A receptors. Agonists must stabilize (one of) the active state of the receptor, and there is no logical necessity that they do this by making the same contacts (Schwartz and Rosenkilde, 1996). Indeed, there is convincing evidence that peptide ligands bind to extracellular loops; however, at least in certain cases, there is also evidence that parts of peptides dip down into the TM domain and contact some of same positions found to be critical for rhodopsin and the amine GPCRs (DeMartino et al., 1994; Macdonald et al., 2000; Gerber et al., 2001). It is likely, however, that structurally dissimilar ligands bind to some extent in different orientations, and these modes of binding can be extremely difficult to predict (Shapiro et al., 2000).

The Second Extracellular Loop

The second extracellular (E2) loop, which connects TM4 and TM5, also contains residues that contact retinal, as evidenced both by visual inspection and by the SASA analysis described above. This loop also contains one of the two highly conserved Cys that are thought to be disulfide-bonded and thus also link the E2 loop to the top of TM3 in rhodopsin and in amine GPCRs (Savarese et al., 1992). The E2 loop dives down into the TM domain and contains two stretches of β-strand, one of which, β4, lays directly over retinal. The E2 loop thus forms a lid over retinal and protects it from the extracellular milieu. Given the high degree of conservation of the amino acids in the β4 strand in vertebrate opsins, and the variability within this region in other class A receptors, it has been suggested that the β4 strand might serve specifically to define the retinal binding-pocket in vertebrate opsins and not other GPCRs (Menon et al., 2001).

The sequence of the E2 loop is highly variable across class A receptors; as we have noted previously, however, the sequence from 4.59 to 4.68 is highly conserved among functionally related receptors and among species variants of these receptors (Javitch et al., 2000). It is likely, therefore, that this region plays a functional role. This inference is supported by the identification of this region as the site of covalent attachment of photoaffinity derivatives of agonist and antagonist ligands of the α_2 adrenergic receptor (Matsui et al., 1989), by the observed ligand-specific effects of mutations in this region (reviewed in Javitch et al., 2000), and by the predicted spatial proximity of this region to known ligand binding sites in other TMs. Thus, although we do not yet know of any structural similarity of the E2 loop between rhodopsin and other class A receptors beyond the shared disulfide bond, there is evidence for an important functional role of this loop in the entire family of receptors. Indeed, in the α_1 adrenergic receptor, Zhao et al. (1996) have demonstrated that several residues in the E2 loop partially determine the pharmacological specificity of particular adrenergic ligands, again suggesting that this loop may contact bound ligands in other Class A receptors in addition to rhodopsin. Remarkably, we have noted that these residues seem to be aligned with the retinal-contact residues in the β4 region of bovine rhodopsin near the disulfide-bond, raising the possibility that there may be some structural similarity in this loop region in other class A receptors and rhodopsin.

Summary

In conclusion, based on our analysis of the data reviewed, the structures of rhodopsin and of amine receptors may be very similar. We further propose that several of the highly unusual structural features of rhodopsin are also present in amine GPCRs, despite the absence of amino acids that might have been thought to be critical to the adoption of these features. Thus, different amino acids or alternate microdomains can support similar deviations from regular α-helical structure, thereby resulting in similar tertiary structure. Such structural mimicry is a mechanism by which a common ancestor could diverge sufficiently to develop the selectivity necessary to interact with diverse signals, while still maintaining a similar overall fold. Through this process, the core

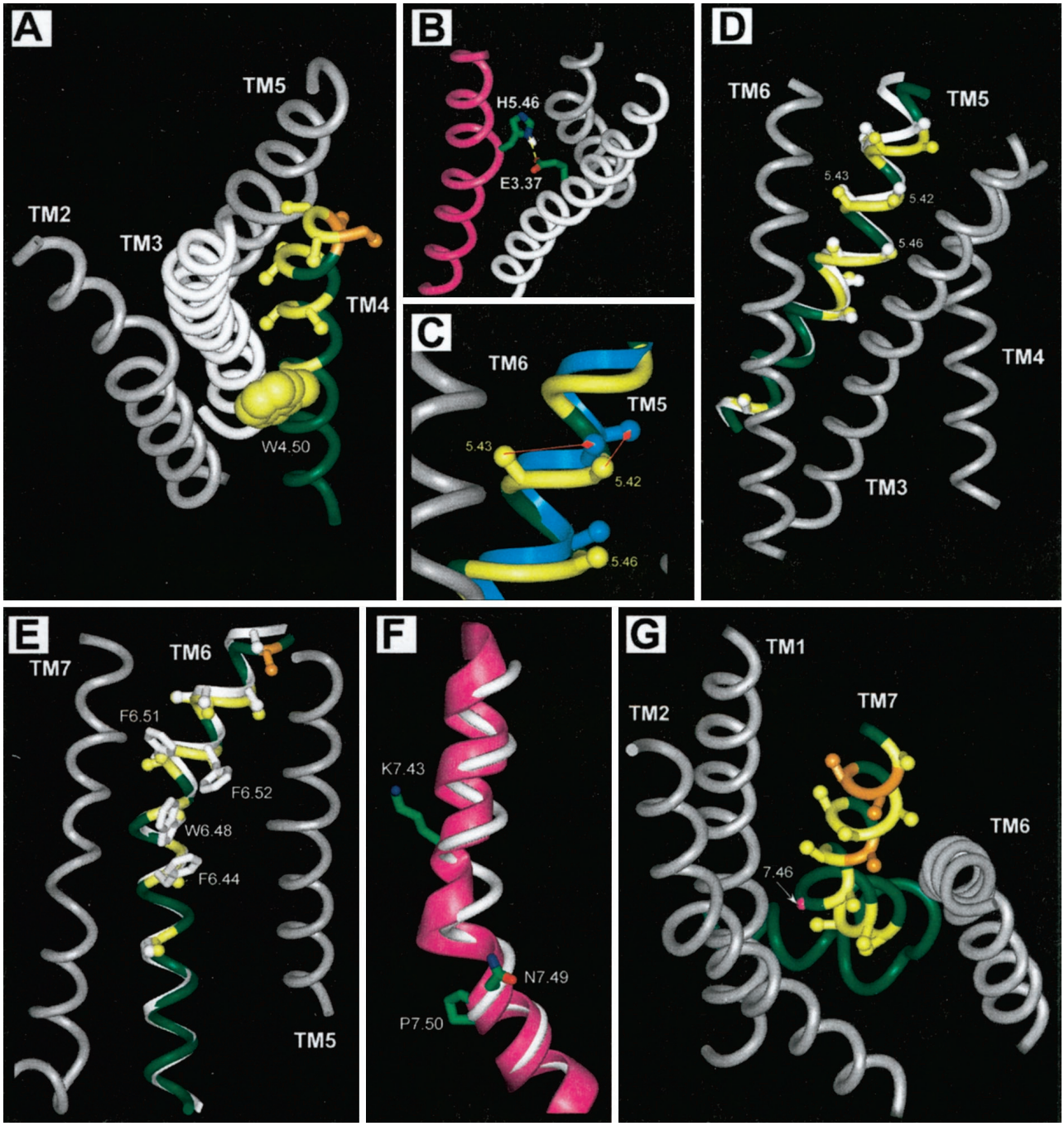

Fig. 6. TM4-TM7. A, three-dimensional molecular representation of TM4 viewed from the extracellular side, in the context of TM2, TM3, and TM5, showing the Cα traces from the high-resolution structure of bovine rhodopsin. The Cα ribbon of TM3 is shown in white; TM2 and TM5 are shown in gray; for TM4, the Cβs of the rhodopsin residues aligned with the accessible D_2 receptor residues are shown in orange. The protected residues are shown in yellow. The remaining residues in TM4 are shown in green without Cβ. The side chain of the highly conserved Trp4.50 is shown in van der Waals representation. B, three-dimensional molecular representation of the interaction between $H211^{5.46}$ of TM5 and $E122^{3.37}$ of TM3 in rhodopsin, in the context of TM2. The top of the panel shows the extracellular end, and the bottom of the panel the intracellular end of the TMs. The Cα ribbon of TM5 is shown in pink; TM3 is shown in white; TM2 is shown in gray. The heavy atoms of side chains with the hydrogen involved in the presumed H-bond of $H211^{5.46}$ and $E122^{3.37}$ are shown by a dashed yellow line. In C, seen from the binding-site crevice, the Cα ribbon of TM5 of rhodopsin and the Pro-kink simulation (see *Materials and Methods*) with the smallest RMSD (blue) is shown with the Cβs of three of the aligned protected residues (5.42 5.43, and 5.46; yellow in TM5 of rhodopsin, and blue in the simulated α-helix). The red lines indicate the relative positions of the Cβ of 5.42 and 5.43 in the best-fit α-helix and in rhodopsin. In D, the Cα ribbons of TM3, TM4, and TM6 are shown in gray; for TM5, the Cβs of the rhodopsin residues aligned with the protected D_2 receptor residues are shown in yellow. The remaining residues in TM5 are shown in green without Cβ. The Cα ribbon of the best-fit (smallest RMSD) α-helix from the Pro/Ser MD simulation (see *Materials and Methods*) is shown with the Cβs of the aligned accessible residues in white. E, three-dimensional molecular representation of TM6, in the context of TM5 and TM7, showing the Cα traces from the high-resolution structure of bovine rhodopsin. The Cα ribbons of TM5 and TM7 are shown in gray; for TM6, the Cβs of the rhodopsin residue aligned with the accessible D_2 receptor residue is shown in orange. The protected residues are shown in yellow. The remaining residues in TM6 are shown in green without Cβ. The Cα ribbon of the best-fit (smallest RMSD) α-helix from the simulation (see *Materials and Methods*) is shown with the Cβs of aligned accessible residues in white. The side chains of the aromatic cluster in D_2 receptor—F6.44, W6.48, F6.51, and F6.52, which are among the protected residues, are shown in white sticks. F, the Cα ribbons of TM7 (pink) with the superimposed best-fit (smallest RMSD) α-helix from the simulation

TABLE 3

Residues in bovine rhodopsin found in SASA calculations to be protected by retinal and aligned residues of representative receptors that have been implicated in ligand binding.

Data are shown as the percentage of total surface of each residue that is exposed to water. All positions listed, except for 3.37, were accessible and protected in D2 receptor SCAM experiments (Javitch et al., 1995a,b, 1998; Fu et al., 1996). Receptor names are abbreviated according to their SWISS-PROT Annotated Protein Sequence Database entry names: http://www.expasy.ch/cgi-bin/lists?7tmrlist.txt

Residues	SASA %			Representative Receptors	References
	NR	WR	Δ		
Glu113$^{3.28}$	0.4	0.0	0.4	D2DR, ACM1, NK2R	Bhogal et al., 1994; Matsui et al., 1995; Simpson et al., 1999
Gly114$^{3.29}$	0.3	0.0	0.3	D2DR, P2YR, GASR, MSHR, ACTR	Kopin et al., 1995; Naville et al., 1996; Jiang et al., 1997; Yang et al., 1997; Simpson et al., 1999
Ala117$^{3.32}$	13.1	2.4	10.7	5H1A, B2AR, A2AA, D2DR, HH2R, ACM1, ETBR	Strader et al., 1987, 1988, 1991; Fraser et al., 1989; Wang et al., 1991; Gantz et al., 1992; Ho et al., 1992; Mansour et al., 1992; Zhu et al., 1992
Thr118$^{3.33}$	15.1	0.0	15.1	ACM3, AA1R	Wess et al., 1991; Rivkees et al., 1999;
Gly121$^{3.36}$	6.1	0.0	6.1	5H2A	Almaula et al., 1996
Glu122$^{3.37}$	10.7	0.0	10.7	AA2A, AA1R, P2YR	Jiang et al., 1996; Moro et al., 1998; Rivkees et al., 1999
Met207$^{5.42}$	10.6	0.3	10.3	5H1A, A2AA, B2AR	Wang et al., 1991; Ho et al., 1992; Liapakis et al., 2000
Phe208$^{5.43}$	7.3	5.0	2.3	D2DR, B2AR	Strader et al., 1989; Mansour et al., 1992
His211$^{5.46}$	1.6	0.5	1.1	A2AA, D2DR, B2AR	Strader et al., 1989; Wang et al., 1991; Mansour et al., 1992
Phe212$^{5.47}$	21.6	14.6	7.0	A1AA, 5H2A, D2DR	Cho et al., 1995; Wetzel et al., 1996; Shapiro et al., 2000
Phe261$^{6.44}$	5.1	0.9	4.2	ET1R	Breu et al., 1995
Trp265$^{6.48}$	13.0	0.5	12.5	5H1B, 5H2A	Roth et al., 1997; Granas and Larhammar, 1999;
Tyr268$^{6.51}$	14.0	0.0	14.0	A1AB	Chen et al., 1999
Ala269$^{6.52}$	14.8	3.1	11.7	5H1B, 5H2A, B2AR	Dixon et al., 1988; Choudhary et al., 1993; Granas et al., 1998
Ala272$^{6.55}$	1.0	0.3	0.7	B2AR, D2DR	Woodward et al., 1994; Wieland et al., 1996
Ala292$^{7.39}$	5.5	0.0	5.5	5H1A, 5H1B, B2AR, A2AA, ACM1, P2UR, GASR, P2YR	Suryanarayana et al., 1991; Guan et al., 1992; Oksenberg et al., 1992; Suryanarayana and Kobilka, 1993; Erb et al., 1995; Kopin et al., 1995; Matsui et al., 1995; Jiang et al., 1997
Ala295$^{7.42a}$	2.6	0.0	2.6	ACM1, AA1R, AG2R, NTR1	Savarese et al., 1992; Tucker et al., 1994; Perlman et al., 1997; Labbe-Jullie et al., 1998
Lys296$^{7.43}$	3.3	0.8	2.5	5H2A, AA2A, AA1R, P2YR, PAFR	Olah et al., 1992; Kim et al., 1995; Ishii et al., 1997; Jiang et al., 1997; Roth et al., 1997

NR, SASA calculated without retinal; WR, SASA calculated with retinal; Δ, difference between NR and WR.
[a] G415$^{7.42}$C in the D2 receptor did not bind ligand.

function of signaling activation through a conformational change in the TMs that alters the conformation of the cytoplasmic surface and subsequent interaction with G-proteins is presumably shared by the entire Class A family of receptors, despite their selectivity for a diverse group of ligands.

It is important to note, however, as we have discussed above, that there are differences in sequence that might result in some extent of divergence in the resulting structure of some Class A receptors. An example of this is the presence of Pro in TM2 at different positions, where they might bend the helix differently (Fig. 5C). Furthermore, a significant range of conformational diversity could be generated within the binding-site crevice of different GPCRs by the presence of Pro-kinks and Cys/Ser/Thr residues. Conserved Pro-kinks in TM 5, 6, and 7 could adopt different conformations that could change significantly the binding sites of different GPCRs. Nonconserved Pro residues in TM 2 and 4, or nonconserved Cys/Ser/Thr in TM 3 and other helices, are another source of potential structural divergence in the binding-site crevice. Combined, these sources of structural diversity may be capable of generating a large diversity of binding site conformations. It seems, therefore, that these receptors have evolved to maintain an overall fold by means of alternative molecular mechanisms (structural mimicry) that enable localized variations within their binding sites suitable for recognizing a wide variety of ligands. This scenario supports the use of the crystal structure of rhodopsin as a template to model the transmembrane domain of other rhodopsin-like GPCRs. The initial template, however, may require substantial modifications to refine the particular conformation of the binding site to explore ligand-receptor interactions at the molecular level.

Materials and Methods

Residue Indexing. To facilitate comparison of aligned residues in related GPCRs, the most conserved residue in TMX is given the index number X.50, and residues within a given TM are then indexed relative to the "50" position (Ballesteros and Weinstein, 1995). The most highly conserved residues in this family are indicated in Fig. 1 in an alignment of rhodopsin with a selected group of class A GPCRs. (Note that the "50" position does not necessitate that the residue is in the "middle" of the TM; e.g., the highly conserved Arg3.50 is at the cytoplasmic end of TM3 in the conserved E/D-R-Y sequence.)

Molecular Dynamics Simulations. To explore the bending of a membrane-spanning α-helix by a single Pro, 100 α-helices of 30 amino acids with a Pro at position 22 from the N terminus and Ala at the other positions were generated by molecular dynamics (MD) simulation with CHARMM (version 27b1) (Brooks et al., 1983). The

(see *Materials and Methods*) (white). The side chain heavy atoms of K7.43 (the attachment site of retinal) and the NP motif (Asn7.49 and Pro7.50) are shown in sticks to illustrate their positions relative to the 3_{10} helix (7.43–7.46). G, three-dimensional molecular representation of TM7, viewed extracellularly, in the context of TM1, TM2, and TM6, showing the Cα traces from the high-resolution structure of bovine rhodopsin. The Cα ribbons of TM1, TM2, and TM6 are shown in gray; for TM7, the Cβs of the rhodopsin residues aligned with the accessible D_2 receptor residues are shown in orange. The protected residues are shown in yellow. The remaining residues in TM7 are shown in green without Cβ. The Cα of 7.46 is indicated in pink.

simulation was started from the torsion angles taken from average values of Pro-kinks, and a dielectric constant of 4 was used. The system was heated to 300°K and equilibrated. After the major parameters were stable in the production phase, a structure was extracted every 2 ps.

The generated α-helices were taken as representative of the potential conformational space accessible to a Pro-kink and were superimposed on the conserved cytoplasmic side of various TMs to align the Pro appropriately (TM2, 1–17 to 2.38–2.54; TM5, 23–30 to 5.51–5.58; TM6, 2–18 to 6.30–6.46; and TM7, 21–25 to 7.49–7.53). The RMSDs were calculated between the coordinates of the Cα atoms of the indicated regions of the simulated α-helices and those in the corresponding regions of rhodopsin: (TM2, 18–30 to 2.55–2.67; TM5, 11–18 to 5.39–5.46; and TM6, 19–30 to 6.47–6.58). To make the simulated α-helices the same length as the superimposed TMs, they were shortened or lengthened by adding Ala residues with ideal α-helix Φ,Ψ values.

A second MD simulation was similarly performed for TM5. An α-helix of 26 amino acids was generated, however, with three serines at positions 8, 9, and 12, in addition to a Pro at position 16. The side chains of serines were restrained in certain rotamers (MIN) by well shaped energy barriers [60° on each side (WIDTH), force constant (FORCE) of 5 kcal/mol/radian^2; the energy of constraint dihedral angle (Ecdih) was calculated by Ecdih = FORCE $\times$ max(0, abs(χ_1 − MIN $\times$ π/180) − WIDTH)^2)]. The Ser at position 8 was placed in the gauche-rotamer, as this was the only rotamer that positioned this residue toward the binding-site crevice where it could participate in its known interactions (see text). The Ser at 9 and 12 were placed in the gauche+, gauche−, or *trans*-rotamers. Simulations were run with each of the possible nine different rotamer combinations. The generated α-helices were superimposed on TM5 (17–24 to 5.51–5.58). The RMSDs were calculated between the coordinates of the Cα atoms of the indicated regions of the simulated α-helices and those in the corresponding region of rhodopsin (TM5, 5–12 to 5.39–5.46).

Modeling of the Cys/Ser/Thr Effects on Helix Backbone. To simulate the possible roles of Cys/Ser/Thr in the distortion of the α-helix backbone, 54 α-helices of 33 amino acids were generated using the average (Φ, Ψ) values of Cys/Ser/Thr when they are in the gauche+ (−63.7, −41.6)/(−63.3, −42.2)/(−63.4, −44.2), gauche− (not populated)/(−66.5, −33.5)/(−69.6, −35.0), and *trans* (−62.0, −46.1)/(−62.7, −44.0)/(−68.8, −40.1) rotamers (Ballesteros et al., 2000), to simulate the possible conformations in the human dopamine D_2 receptor, which contains Thr3.37, Ser3.39, Cys3.44, and Ser3.47.

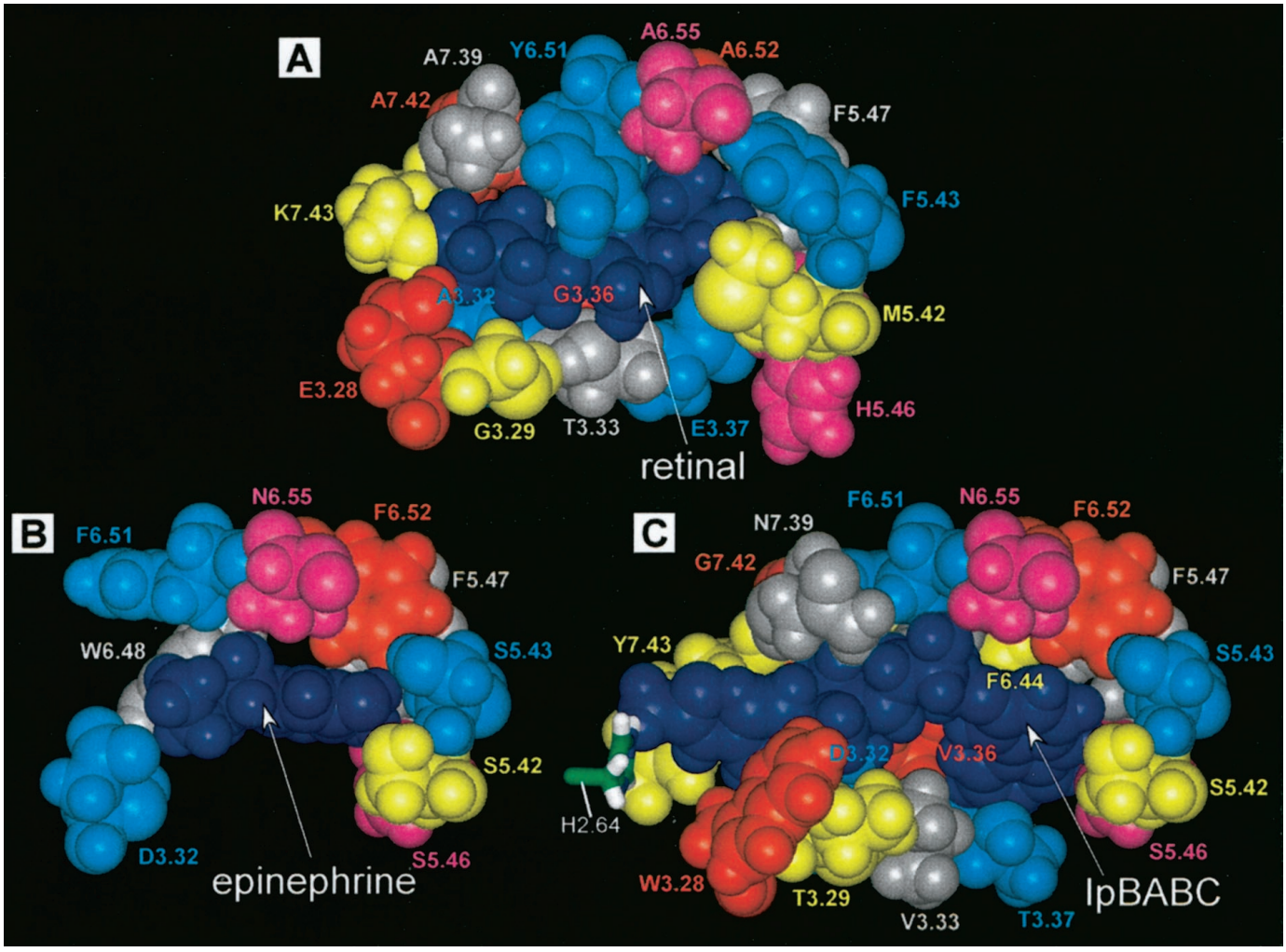

Fig. 7. Ligand binding crevice. A, the residues in the TMs that were identified from the SASA analysis (see text and Table 3) are shown in van der Waals representation, with retinal bound within the surface created by these residues. B, the side chains of residues from the β_2 adrenergic receptor are shown on the backbone of the rhodopsin structure. These residues have been experimentally determined to interact with catecholamine ligands, and include Asp113$^{3.32}$, Ser203$^{5.42}$, Ser204$^{5.43}$, Ser207$^{5.46}$, Phe208$^{5.47}$, Trp286$^{6.48}$, Phe289$^{6.51}$, Phe290$^{6.52}$, and Asn293$^{6.55}$, a subset of the positions shown in A. C, IpBABC, an affinity-labeled derivative of pindolol, is docked within the TMs of the rhodopsin structure with all the residues from Table 3 mutated to the aligned β_2 adrenergic receptor residues. IpBABC is shown covalently attached to His93$^{2.64}$ in TM2. Residues with the same index number are shown in the same color in all three panels. The residues displayed next to each other are shown in different colors.

Acknowledgments

We are grateful to Arthur Karlin for helpful discussion and to Harel Weinstein for helpful discussion, for comments on the manuscript and for suggesting the term "mimicry" to convey our thesis.

References

Akabas MH, Stauffer DA, Xu M and Karlin A (1992) Acetylcholine receptor channel structure probed in cysteine-substitution mutants. *Science (Wash DC)* **258:**307–310.

Albert AD and Yeagle PL (2000) Domain approach to three-dimensional structure of rhodopsin using high-resolution nuclear magnetic resonance. *Methods Enzymol* **315:**107–115.

Almaula N, Ebersole BJ, Zhang D, Weinstein H and Sealfon SC (1996) Mapping the binding site pocket of the serotonin 5-Hydroxytryptamine2A receptor. Ser3.36(159) provides a second interaction site for the protonated amine of serotonin but not of lysergic acid diethylamide or bufotenin. *J Biol Chem* **271:**14672–14675.

Altenbach C, Cai K, Khorana HG and Hubbell WL (1999a) Structural features and light-dependent changes in the sequence 306–322 extending from helix VII to the palmitoylation sites in rhodopsin: a site-directed spin-labeling study. *Biochemistry* **38:**7931–7937.

Altenbach C, Klein-Seetharaman J, Hwa J, Khorana HG and Hubbell WL (1999b) Structural features and light-dependent changes in the sequence 59–75 connecting helices I and II in rhodopsin: a site-directed spin-labeling study. *Biochemistry* **38:**7945–7949.

Altenbach C, Yang K, Farrens DL, Farahbakhsh ZT, Khorana HG and Hubbell WL (1996) Structural features and light-dependent changes in the cytoplasmic interhelical E-F loop region of rhodopsin: a site-directed spin-labeling study. *Biochemistry* **35:**12470–12478.

Baldwin JM, Schertler GF and Unger VM (1997) An α-carbon template for the transmembrane helices in the rhodopsin family of G-protein-coupled receptors. *J Mol Biol* **272:**144–164.

Ballesteros J and Weinstein H (1995) Integrated methods for the construction of three-dimensional models of structure-function relations in G protein-coupled receptors. *Methods Neurosci* **25:**366–428.

Ballesteros JA, Deupi X, Olivella M, Haaksma EE and Pardo L (2000) Serine and threonine residues bend α-helices in the chi(1) = g(−) conformation. *Biophys J* **79**:2754–2760.

Ballesteros JA, Jensen AD, Liapakis G, Rasmussen SG, Shi L, Gether U and Javitch JA (2001) Activation of the β_2 adrenergic receptor involves disruption of an ionic lock between the cytoplasmic ends of transmembrane segments 3 and 6. *J Biol Chem*, in press.

Ballesteros JA and Weinstein H (1992) Analysis and refinement of criteria for predicting the structure and relative orientations of transmembranal helical domains. *Biophys J* **62:**107–109.

Barlow DJ and Thornton JM (1988) Helix geometry in proteins. *J Mol Biol* **201:**601–619.

Beck M, Sakmar TP and Siebert F (1998) Spectroscopic evidence for interaction between transmembrane helices 3 and 5 in rhodopsin. *Biochemistry* **37:**7630–7639.

Bhogal N, Donnelly D and Findlay JB (1994) The ligand binding site of the neurokinin 2 receptor. Site-directed mutagenesis and identification of neurokinin A binding residues in the human neurokinin 2 receptor. *J Biol Chem* **269:**27269–27274.

Breu V, Hashido K, Broger C, Miyamoto C, Furuichi Y, Hayes A, Kalina B, Loffler BM, Ramuz H and Clozel M (1995) Separable binding sites for the natural agonist endothelin-1 and the non-peptide antagonist bosentan on human endothelin-A receptors. *Eur J Biochem* **231:**266–270.

Brooks BR, Bruccoleri RE, Olafson BD, States DJ, Swaminathan S and Karplus M (1983) CHARMM: A program for macromolecular energy, minimization, and dynamics calculations. *J Comp Chem* **4:**187–217.

Chen S, Xu M, Lin F, Lee D, Riek P and Graham RM (1999) Phe310 in transmembrane VI of the α_{1B}-adrenergic receptor is a key switch residue involved in activation and catecholamine ring aromatic bonding. *J Biol Chem* **274:**16320–16330.

Cho W, Taylor LP, Mansour A and Akil H (1995) Hydrophobic residues of the D_2 dopamine receptor are important for binding and signal transduction. *J Neurochem* **65:**2105–2115.

Choudhary MS, Craigo S and Roth BL (1993) A single point mutation (Phe340–>Leu340) of a conserved phenylalanine abolishes 4-[^{125}I]iodo-(2,5-dimethoxy)phenylisopropylamine and [^{3}H]mesulergine but not [3H]ketanserin binding to 5-hydroxytryptamine2 receptors. *Mol Pharmacol* **43:**755–761.

Choudhary MS, Sachs N, Uluer A, Glennon RA, Westkaemper RB and Roth BL (1995) Differential ergoline and ergopeptine binding to 5-hydroxytryptamine2A receptors: ergolines require an aromatic residue at position 340 for high affinity binding. *Mol Pharmacol* **47:**450–457.

Colson AO, Perlman JH, Smolyar A, Gershengorn MC and Osman R (1998) Static and dynamic roles of extracellular loops in G-protein-coupled receptors: a mechanism for sequential binding of thyrotropin-releasing hormone to its receptor. *Biophys J* **74:**1087–100.

DeMartino JA, Van Riper G, Siciliano SJ, Molineaux CJ, Konteatis ZD, Rosen H and Springer MS (1994) The amino terminus of the human C5a receptor is required for high affinity C5a binding and for receptor activation by C5a but not C5a analogs. *J Biol Chem* **269:**14446–14450.

Dixon RA, Sigal IS and Strader CD (1988) Structure-function analysis of the β-adrenergic receptor. *Cold Spring Harb Symp Quant Biol* **53:**487–497.

Dohlman HG, Caron MG, Strader CD, Amlaiky N and Lefkowitz RJ (1988) Identification and sequence of a binding site peptide of the β_2-adrenergic receptor. *Biochemistry* **27:**1813–1817.

Elling CE, Nielsen SM and Schwartz TW (1995) Conversion of antagonist-binding site to metal-ion site in the tachykinin NK-1 receptor. *Nature (Lond)* **374:**74–77.

Elling CE and Schwartz TW (1996) Connectivity and orientation of the seven helical bundle in the tachykinin NK-1 receptor probed by zinc site engineering. *EMBO J* **15:**6213–6219.

Elling CE, Thirstrup K, Holst B and Schwartz TW (1999) Conversion of agonist site to metal-ion chelator site in the β_2-adrenergic receptor. *Proc Natl Acad Sci U S A* **96:**12322–12327.

Elling CE, Thirstrup K, Nielsen SM, Hjorth SA and Schwartz TW (1997) Metal-ion sites as structural and functional probes of helix-helix interactions in 7TM receptors. *Ann N Y Acad Sci* **814:**142–151.

Erb L, Garrad R, Wang Y, Quinn T, Turner JT and Weisman GA (1995) Site-directed mutagenesis of P2U purinoceptors. Positively charged amino acids in transmembrane helices 6 and 7 affect agonist potency and specificity. *J Biol Chem* **270:**4185–4188.

Farahbakhsh ZT, Ridge KD, Khorana HG and Hubbell WL (1995) Mapping light-dependent structural changes in the cytoplasmic loop connecting helices C and D in rhodopsin: a site-directed spin labeling study. *Biochemistry* **34:**8812–8819.

Farrens DL, Altenbach C, Yang K, Hubbell WL and Khorana HG (1996) Requirement of rigid-body motion of transmembrane helices for light activation of rhodopsin. *Science (Wash DC)* **274:**768–770.

Findlay JB, Barclay PL, Brett M, Davison M, Pappin DJ and Thompson P (1984) The structure of mammalian rod opsins. *Vision Res* **24:**1501–1508.

Fraser CM, Wang CD, Robinson DA, Gocayne JD and Venter JC (1989) Site-directed mutagenesis of m1 muscarinic acetylcholine receptors: conserved aspartic acids play important roles in receptor function. *Mol Pharmacol* **36:**840–847.

Fu D, Ballesteros JA, Weinstein H, Chen J and Javitch JA (1996) Residues in the seventh membrane-spanning segment of the dopamine D_2 receptor accessible in the binding-site crevice. *Biochemistry* **35:**11278–11285.

Gantz I, DelValle J, Wang LD, Tashiro T, Munzert G, Guo YJ, Konda Y and Yamada T (1992) Molecular basis for the interaction of histamine with the histamine H2 receptor. *J Biol Chem* **267:**20840–20843.

Gerber BO, Meng EC, Dotsch V, Baranski TJ and Bourne HR (2001) An activation switch in the ligand binding pocket of the C5a receptor. *J Biol Chem* **276:**3394–3400.

Gether U (2000) Uncovering molecular mechanisms involved in activation of G protein-coupled receptors. *Endocr Rev* **21:**90–113.

Gibson NJ and Brown MF (1993) Lipid headgroup and acyl chain composition modulate the MI-MII equilibrium of rhodopsin in recombinant membranes. *Biochemistry* **32:**2438–2454.

Gouldson PR, Snell CR and Reynolds CA (1997) A new approach to docking in the β_2-adrenergic receptor that exploits the domain structure of G-protein-coupled receptors. *J Med Chem* **40:**3871–3886.

Govaerts C, Blanpain C, Deupi X, Ballet S, Ballesteros JA, Wodak SJ, Vassart G, Pardo L and Parmentier M (2001) The TxP motif in the second transmembrane helix of CCR5: a structural determinant of chemokine-induced activation. *J Biol Chem*, in press.

Granas C and Larhammar D (1999) Identification of an amino acid residue important for binding of methiothepin and sumatriptan to the human 5-HT(1B) receptor. *Eur J Pharmacol* **380:**171–181.

Granas C, Nordvall G and Larhammar D (1998) Mutagenesis of the human 5-HT1B receptor: differences from the closely related 5-HT1A receptor and the role of residue F331 in signal transduction. *J Recept Signal Transduct Res* **18:**225–241.

Gray TM and Matthews BW (1984) Intrahelical hydrogen bonding of serine, threonine and cysteine residues within α-helices and its relevance to membrane-bound proteins. *J Mol Biol* **175:**75–81.

Guan XM, Peroutka SJ and Kobilka BK (1992) Identification of a single amino acid residue responsible for the binding of a class of β-adrenergic receptor antagonists to 5-hydroxytryptamine1A receptors. *Mol Pharmacol* **41:**695–698.

Han M, Lin SW, Minkova M, Smith SO and Sakmar TP (1996) Functional interaction of transmembrane helices 3 and 6 in rhodopsin. Replacement of phenylalanine 261 by alanine causes reversion of phenotype of a glycine 121 replacement mutant. *J Biol Chem* **271:**32337–32342.

Hardy JA, Walsh ST and Nelson HC (2000) Role of an α-helical bulge in the yeast heat shock transcription factor. *J Mol Biol* **295:**393–409.

Inooka H, Ohtaki T, Kitahara O, Ikegami T, Endo S, Kitada C, Ogi K, Onda H, Fujino M and Shirakawa M (2001) Conformation of a peptide ligand bound to its G-protein coupled receptor. *Nat Struct Biol* **8:**161–165.

Ishii I, Izumi T, Tsukamoto H, Umeyama H, Ui M and Shimizu T (1997) Alanine exchanges of polar amino acids in the transmembrane domains of a platelet-activating factor receptor generate both constitutively active and inactive mutants. *J Biol Chem* **272:**7846–7854.

Javitch JA, Ballesteros JA, Chen J, Chiappa V and Simpson MM (1999) Electrostatic and aromatic microdomains within the binding-site crevice of the D_2 receptor: contributions of the second membrane-spanning segment. *Biochemistry* **38:**7961–7968.

Javitch JA, Ballesteros JA, Weinstein H and Chen J (1998) A cluster of aromatic residues in the sixth membrane-spanning segment of the dopamine D_2 receptor is accessible in the binding-site crevice. *Biochemistry* **37:**998–1006.

Javitch JA, Fu D and Chen J (1995a) Residues in the fifth membrane-spanning segment of the dopamine D_2 receptor exposed in the binding-site crevice. *Biochemistry* **34:**16433–16439.

Javitch JA, Fu D, Chen J and Karlin A (1995b) Mapping the binding-site crevice of the dopamine D_2 receptor by the substituted-cysteine accessibility method. *Neuron* **14:**825–831.

Javitch JA, Li X, Kaback J and Karlin A (1994) A cysteine residue in the third membrane-spanning segment of the human D_2 dopamine receptor is exposed in the binding-site crevice. *Proc Natl Acad Sci USA* **91:**10355–10359.

Javitch JA, Shi L and Liapakis G (2001) Use of the substituted-cysteine accessibility method (SCAM) to study the structure and function of G-protein-coupled receptors. *Methods Enzymol*, in press.
Javitch JA, Shi L, Simpson MM, Chen J, Chiappa V, Visiers I, Weinstein H and Ballesteros JA (2000) The fourth transmembrane segment of the dopamine D_2 receptor: accessibility in the binding-site crevice and position in the transmembrane bundle. *Biochemistry* **39:**12190–12199.
Jensen AD, Guarnieri F, Rasmussen SG, Asmar F, Ballesteros JA and Gether U (2000) Agonist-induced conformational changes at the cytoplasmic side of TM 6 in the β_2 adrenergic receptor mapped by site-selective fluorescent labeling. *J Biol Chem* **276:**9279–9290.
Jiang Q, Guo D, Lee BX, Van Rhee AM, Kim YC, Nicholas RA, Schachter JB, Harden TK and Jacobson KA (1997) A mutational analysis of residues essential for ligand recognition at the human P2Y1 receptor. *Mol Pharmacol* **52:**499–507.
Jiang Q, Van Rhee AM, Kim J, Yehle S, Wess J and Jacobson KA (1996) Hydrophilic side chains in the third and seventh transmembrane helical domains of human A2A adenosine receptors are required for ligand recognition. *Mol Pharmacol* **50:**512–521.
Jornvall H, Persson B, Krook M, Atrian S, Gonzalez-Duarte R, Jeffery J and Ghosh D (1995) Short-chain dehydrogenases/reductases (SDR). *Biochemistry* **34:**6003–6013.
Karlin A and Akabas MH (1998) Substituted-cysteine accessibility method. *Methods Enzymol* **293:**123–145.
Kim J, Wess J, van Rhee AM, Schoneberg T and Jacobson KA (1995) Site-directed mutagenesis identifies residues involved in ligand recognition in the human A2a adenosine receptor. *J Biol Chem* **270:**13987–13997.
Kopin AS, McBride EW, Quinn SM, Kolakowski LF Jr and Beinborn M (1995) The role of the cholecystokinin-B/gastrin receptor transmembrane domains in determining affinity for subtype-selective ligands. *J Biol Chem* **270:**5019–5023.
Kumar S and Bansal M (1998) Geometrical and sequence characteristics of α-helices in globular proteins. *Biophys J* **75:**1935–1944.
Labbe-Jullie C, Barroso S, Nicolas-Eteve D, Reversat JL, Botto JM, Mazella J, Bernassau JM and Kitabgi P (1998) Mutagenesis and modeling of the neurotensin receptor NTR1. Identification of residues that are critical for binding SR 4 8692, a nonpeptide neurotensin antagonist. *J Biol Chem* **273:**16351–16357.
Lee B and Richards FM (1971) The interpretation of protein structures: estimation of static accessibility. *J Mol Biol* **55:**379–400.
Liapakis G, Ballesteros JA, Papachristou S, Chan WC, Chen X and Javitch JA (2000) The forgotten serine. A critical role for Ser-203(5.42) in ligand binding to and activation of the β_2-adrenergic receptor. *J Biol Chem* **275:**37779–37788.
Lin SW, Han M and Sakmar TP (2000) Analysis of functional microdomains of rhodopsin. *Methods Enzymol* **315:**116–130.
Liu J, Schoneberg T, van Rhee M and Wess J (1995) Mutational analysis of the relative orientation of transmembrane helices I and VII in G protein-coupled receptors. *J Biol Chem* **270:**19532–19539.
Lu ZL and Hulme EC (2000) A network of conserved intramolecular contacts defines the off-state of the transmembrane switch mechanism in a seven-transmembrane receptor. *J Biol Chem* **275,** 5682–5686.
Macdonald D, Murgolo N, Zhang R, Durkin JP, Yao X, Strader CD and Graziano MP (2000) Molecular characterization of the melanin-concentrating hormone/receptor complex: identification of critical residues involved in binding and activation. *Mol Pharmacol* **58:**217–225.
Mansour A, Meng F, Meador-Woodruff JH, Taylor LP, Civelli O and Akil H (1992) Site-directed mutagenesis of the human dopamine D_2 receptor. *Eur J Pharmacol* **227:**205–214.
Matsui H, Lazareno S and Birdsall NJ (1995) Probing of the location of the allosteric site on m1 muscarinic receptors by site-directed mutagenesis. *Mol Pharmacol* **47:**88–98.
Matsui H, Lefkowitz RJ, Caron MG and Regan JW (1989) Localization of the fourth membrane spanning domain as a ligand binding site in the human platelet α_2-adrenergic receptor. *Biochemistry* **28:**4125–4130.
Menon ST, Han M and Sakmar TP (2001) Rhodopsin: the structural basis of molecular physiology. *Physiol Rev*, in press.
Mirny LA and Shakhnovich EI (1999) Universally conserved positions in protein folds: reading evolutionary signals about stability, folding kinetics and function. *J Mol Biol* **291:**177–196.
Mizobe T, Maze M, Lam V, Suryanarayana S and Kobilka BK (1996) Arrangement of transmembrane domains in adrenergic receptors. Similarity to bacteriorhodopsin. *J Biol Chem* **271:**2387–2389.
Moro S, Guo D, Camaioni E, Boyer JL, Harden TK and Jacobson KA (1998) Human P2Y1 receptor: molecular modeling and site-directed mutagenesis as tools to identify agonist and antagonist recognition sites. *J Med Chem* **41:**1456–1466.
Naville D, Barjhoux L, Jaillard C, Faury D, Despert F, Esteva B, Durand P, Saez JM and Begeot M (1996) Demonstration by transfection studies that mutations in the adrenocorticotropin receptor gene are one cause of the hereditary syndrome of glucocorticoid deficiency. *J Clin Endocrinol Metab* **81:**1442–1448.
Oksenberg D, Marsters SA, O'Dowd BF, Jin H, Havlik S, Peroutka SJ and Ashkenazi A (1992) A single amino-acid difference confers major pharmacological variation between human and rodent 5-HT1B receptors. *Nature (Lond)* **360:**161–163.
Olah ME, Ren H, Ostrowski J, Jacobson KA and Stiles GL (1992) Cloning, expression, and characterization of the unique bovine A1 adenosine receptor. Studies on the ligand binding site by site-directed mutagenesis. *J Biol Chem* **267:**10764–10770.
Oprian DD (1992) The ligand-binding domain of rhodopsin and other G protein-linked receptors. *J Bioenerg Biomembr* **24:**211–217.
Palczewski K, Kumasaka T, Hori T, Behnke CA, Motoshima H, Fox BA, Le Trong I, Teller DC, Okada T, Stenkamp RE, et al. (2000) Crystal structure of rhodopsin: a G protein-coupled receptor. *Science (Wash DC)* **289:**739–745.
Perlman S, Costa-Neto CM, Miyakawa AA, Schambye HT, Hjorth SA, Paiva AC, Rivero RA, Greenlee WJ and Schwartz TW (1997) Dual agonistic and antagonistic property of nonpeptide angiotensin AT1 ligands: susceptibility to receptor mutations. *Mol Pharmacol* **51:**301–311.
Rao VR, Cohen GB and Oprian DD (1994) Rhodopsin mutation G90D and a molecular mechanism for congenital night blindness. *Nature (Lond)* **367:**639–642.
Rivkees SA, Barbhaiya H and AP IJ (1999) Identification of the adenine binding site of the human A1 adenosine receptor. *J Biol Chem* **274:**3617–3621.
Roberts DD, Lewis SD, Ballou DP, Olson ST and Shafer JA (1986) Reactivity of small thiolate anions and cysteine-25 in papain toward methyl methanethiosulfonate. *Biochemistry* **25:**5595–5601.
Roth BL, Shoham M, Choudhary MS and Khan N (1997) Identification of conserved aromatic residues essential for agonist binding and second messenger production at 5-hydroxytryptamine2A receptors. *Mol Pharmacol* **52:**259–266.
Russell RB and Barton GJ (1994) Structural features can be unconserved in proteins with similar folds. An analysis of side-chain to side-chain contacts secondary structure and accessibility. *J Mol Biol* **244:**332–350.
Sankararamakrishnan R and Vishveshwara S (1992) Geometry of proline-containing α-helices in proteins. *Int J Pept Protein Res* **39:**356–363.
Sansom MS and Weinstein H (2000) Hinges, swivels and switches: the role of prolines in signalling via transmembrane α-helices. *Trends Pharmacol Sci* **21:**445–451.
Savarese TM, Wang CD and Fraser CM (1992) Site-directed mutagenesis of the rat m1 muscarinic acetylcholine receptor. Role of conserved cysteines in receptor function. *J Biol Chem* **267:**11439–11448.
Schwartz TW and Rosenkilde MM (1996) Is there a 'lock' for all agonist 'keys' in 7TM receptors? *Trends Pharmacol Sci* **17:**213–216.
Schwyzer R (1995) 100 years lock-and-key concept: are peptide keys shaped and guided to their receptors by the target cell membrane? *Biopolymers* **37:**5–16.
Sealfon SC, Chi L, Ebersole BJ, Rodic V, Zhang D, Ballesteros JA and Weinstein H (1995) Related contribution of specific helix 2 and 7 residues to conformational activation of the serotonin 5-HT2A receptor. *J Biol Chem* **270:**16683–16688.
Shapiro DA, Kristiansen K, Kroeze WK and Roth BL (2000) Differential modes of agonist binding to 5-Hydroxytryptamine$_{2A}$ serotonin receptors revealed by mutation and molecular modeling of conserved residues in transmembrane region 5. *Mol Pharmacol* **58:**877–886.
Sheikh SP, Vilardarga JP, Baranski TJ, Lichtarge O, Iiri T, Meng EC, Nissenson RA and Bourne HR (1999) Similar structures and shared switch mechanisms of the β_2-adrenoceptor and the parathyroid hormone receptor. Zn(II) bridges between helices III and VI block activation. *J Biol Chem* **274:**17033–17041.
Sheikh SP, Zvyaga TA, Lichtarge O, Sakmar TP and Bourne HR (1996) Rhodopsin activation blocked by metal-ion-binding sites linking transmembrane helices C and F. *Nature (Lond)* **383:**347–350.
Shrake A and Rupley JA (1973) Environment and exposure to solvent of protein atoms. Lysozyme and insulin. *J Mol Biol* **79:**351–371.
Simpson MM, Ballesteros JA, Chiappa V, Chen J, Suehiro M, Hartman DS, Godel T, Snyder LA, Sakmar TP and Javitch JA (1999) Dopamine D4/D2 receptor selectivity is determined by a divergent aromatic microdomain contained within the second, third, and seventh membrane-spanning segments. *Mol Pharmacol* **56:**1116–1126.
Strader CD, Candelore MR, Hill WS, Sigal IS and Dixon RA (1989) Identification of two serine residues involved in agonist activation of the β-adrenergic receptor. *J Biol Chem* **264:**13572–13578.
Strader CD, Gaffney T, Sugg EE, Candelore MR, Keys R, Patchett AA and Dixon RA (1991) Allele-specific activation of genetically engineered receptors. *J Biol Chem* **266:**5–8.
Strader CD, Sigal IS, Candelore MR, Rands E, Hill WS and Dixon RA (1988) Conserved aspartic acid residues 79 and 113 of the β-adrenergic receptor have different roles in receptor function. *J Biol Chem* **263:**10267–10271.
Strader CD, Sigal IS, Register RB, Candelore MR, Rands E and Dixon RA (1987) Identification of residues required for ligand binding to the β-adrenergic receptor. *Proc Natl Acad Sci U S A* **84:**4384–4388.
Struthers M, Yu H, Kono M and Oprian DD (1999) Tertiary interactions between the fifth and sixth transmembrane segments of rhodopsin. *Biochemistry* **38:**6597–6603.
Struthers M, Yu H and Oprian DD (2000) G protein-coupled receptor activation: analysis of a highly constrained, "straitjacketed" rhodopsin. *Biochemistry* **39:**7938–7942.
Suryanarayana S, Daunt DA, Von Zastrow M and Kobilka BK (1991) A point mutation in the seventh hydrophobic domain of the α_2 adrenergic receptor increases its affinity for a family of β receptor antagonists. *J Biol Chem* **266:**15488–15492.
Suryanarayana S and Kobilka BK (1993) Amino acid substitutions at position 312 in the seventh hydrophobic segment of the β_2-adrenergic receptor modify ligand-binding specificity. *Mol Pharmacol* **44:**111–114.
Tucker AL, Robeva AS, Taylor HE, Holeton D, Bockner M, Lynch KR and Linden J (1994) A1 adenosine receptors. Two amino acids are responsible for species differences in ligand recognition. *J Biol Chem* **269:**27900–27906.
Unger VM, Hargrave PA, Baldwin JM and Schertler GF (1997) Arrangement of rhodopsin transmembrane α-helices. *Nature (Lond)* **389:**203–206.
Visiers I, Ballesteros JA and Weinstein H (2001) Computational methods for the construction and analysis of three dimensional representations of GPCR structures and mechanisms. *Methods Enzymol*, in press.
Wang CD, Buck MA and Fraser CM (1991) Site-directed mutagenesis of α_{2A}-adrenergic receptors: identification of amino acids involved in ligand binding and receptor activation by agonists. *Mol Pharmacol* **40:**168–179.
Wess J, Gdula D and Brann MR (1991) Site-directed mutagenesis of the m3 muscarinic receptor: identification of a series of threonine and tyrosine residues involved in agonist but not antagonist binding. *EMBO J* **10:**3729–3734.
Wetzel JM, Salon JA, Tamm JA, Forray C, Craig D, Nakanishi H, Cui W, Vaysse PJ, Chiu G, Weinshank RL, et al. (1996) Modeling and mutagenesis of the human

α_{1A}-adrenoceptor: orientation and function of transmembrane helix V sidechains. *Recept Channels* **4:**165–177.
White SH and Wimley WC (1999) Membrane protein folding and stability: physical principles. *Annu Rev Biophys Biomol Struct* **28:**319–365.
Wieland K, Zuurmond HM, Krasel C, IJzerman AP and Lohse MJ (1996) Involvement of Asn-293 in stereospecific agonist recognition and in activation of the β_2-adrenergic receptor. *Proc Natl Acad Sci U S A* **93:**9276–9281.
Wilson CA, Kreychman J and Gerstein M (2000) Assessing annotation transfer for genomics: quantifying the relations between protein sequence, structure and function through traditional and probabilistic scores. *J Mol Biol* **297:**233–249.
Woodward R, Daniell SJ, Strange PG and Naylor LH (1994) Structural studies on D_2 dopamine receptors: mutation of a histidine residue specifically affects the binding of a subgroup of substituted benzamide drugs. *J Neurochem* **62:**1664–1669.
Yang AS and Honig B (2000a) An integrated approach to the analysis and modeling of protein sequences and structures. II. On the relationship between sequence and structural similarity for proteins that are not obviously related in sequence. *J Mol Biol* **301:**679–689.
Yang AS and Honig B (2000b) An integrated approach to the analysis and modeling of protein sequences and structures. III. A comparative study of sequence conservation in protein structural families using multiple structural alignments. *J Mol Biol* **301:**691–711.
Yang DP, Mavromoustakos T, Beshah K and Makriyannis A (1992) Amphipathic interactions of cannabinoids with membranes. A comparison between delta 8-THC and its O-methyl analog using differential scanning calorimetry, X-ray diffraction and solid state 2H-NMR. *Biochim Biophys Acta* **1103:**25–36.
Yang K, Farrens DL, Altenbach C, Farahbakhsh ZT, Hubbell WL and Khorana HG (1996) Structure and function in rhodopsin. Cysteines 65 and 316 are in proximity in a rhodopsin mutant as indicated by disulfide formation and interactions between attached spin labels. *Biochemistry* **35:**14040–14046.
Yang Y, Dickinson C, Haskell-Luevano C and Gantz I (1997) Molecular basis for the interaction of [Nle4,D-Phe7]melanocyte stimulating hormone with the human melanocortin-1 receptor. *J Biol Chem* **272:**23000–10.
Yu H, Kono M and Oprian DD (1999) State-dependent disulfide cross-linking in rhodopsin. *Biochemistry* **38:**12028–12032.
Yu H and Oprian DD (1999) Tertiary interactions between transmembrane segments 3 and 5 near the cytoplasmic side of rhodopsin. *Biochemistry* **38:**12033–12040.
Zeng FY, Hopp A, Soldner A and Wess J (1999) Use of a disulfide cross-linking strategy to study muscarinic receptor structure and mechanisms of activation. *J Biol Chem* **274:**16629–16640.
Zhao MM, Hwa J and Perez DM (1996) Identification of critical extracellular loop residues involved in α_1-adrenergic receptor subtype-selective antagonist binding. *Mol Pharmacol* **50:**1118–1126.
Zhou W, Flanagan C, Ballesteros JA, Konvicka K, Davidson JS, Weinstein H, Millar RP and Sealfon SC (1994) A reciprocal mutation supports helix 2 and helix 7 proximity in the gonadotropin-releasing hormone receptor. *Mol Pharmacol* **45:**165–170.
Zhu G, Wu LH, Mauzy C, Egloff AM, Mirzadegan T and Chung FZ (1992) Replacement of lysine-181 by aspartic acid in the third transmembrane region of endothelin type B receptor reduces its affinity to endothelin peptides and sarafotoxin 6c without affecting G protein coupling. *J Cell Biochem* **50:**159–164.

Address correspondence to: Dr. Jonathan A. Javitch, Center for Molecular Recognition, Columbia University, P & S 11–401, 630 West 168th Street, New York, NY 10032. E-mail: jaj2@columbia.edu